Calibration of Electronic Components for the Radio Neutrino Observatory in Greenland (RNO-G)

Bachelorarbeit aus der Physik

Vorgelegt von
Nico Neumüller
August 17, 2024

Friedrich-Alexander-Universität Erlangen-Nürnberg

Betreuer: PD Dr. Robert Lahmann

Abstract

The objective of this work is to analyze the reproducibility of the calibration measurements of the radio hardware for the Radio Neutrino Observatory in Greenland (RNO-G). This was done by repeatedly measuring the S-parameters of the transmission chain that transmits the radio signal from the antennas in the ice to the data acquisition systems on the surface. These were analyzed for dependence on environmental variables such as supply voltage and the influence of connectors. Differences between different surface signal amplifiers (DRAB boards) were also investigated. During the measurements, the calibration of the Vector Network Analyzer, which has been used for the measurements, was improved. An influence of the fiber connector on the S-parameters could be determined, while supply voltage fluctuations had no influence on the S-parameters.

Contents

1. Introduction

In this work the reproducibility of the calibration of RNO-G (Radio Neutrino Observatory in Greenland) radio hardware, more precise of the IGLU[1]-Fiber-DRAB[2] chain will be analyzed. First it will be discussed why high-energy neutrinos are well suited as messenger particles for astrophysical processes. Subsequently, the technique of radio detection will be discussed and the Radio Neutrino Observatory in Greenland (RNO-G) will be described.

1.1. Neutrinos as messenger particles

Many astronomical objects are thought to be sources of high-energy neutrinos, such as supernovae, supernova remnants (SNR) or active galactic nuclei (AGN). Neutrino astronomy could lead to a better understanding of these objects. It is assumed that high-energy neutrinos are created in these objects by the decay of particles, which in turn are created by interactions of high-energy charged particles with surrounding matter.
Another source of ultra-high-energy neutrinos could be the GZK (Greisen-Zatsepin-Kuzmin) effect as described in [8]. The GZK effect describes the absorption of ultra-high-energy protons by interactions with photons of the Cosmic Microwave Background (CMB), preventing the long-distance propagation of ultra-high-energy protons. The interactions produce pions, which can decay into ultra-high-energy "cosmogenic" neutrinos. Finding neutrinos from this process is one of the main goals of radio neutrino observatories like RNO-G.

Neutrinos have several advantages over "classical" astrophysical messenger particles. In opposite to cosmic rays they do not carry electrical charge, they are not influenced by magnetic fields via the Lorentz force. Interstellar magnetic fields, which are not yet well understood, currently make it impossible or at least difficult to find the sources of charged cosmic rays. Opposite to this, neutrinos propagate strait, making it is possible to determine the direction of origin.
The most important messenger particles in the high-energy range are still the gamma photons, in the sense that more sources are known and the underlying particle-physical properties are better understood. The main disadvantage of electromagnetic radiation is, it can be absorbed quite easily, e.g. in dense molecular clouds. Since neutrinos do only interact via the weak interaction, their absorption cross-section is small and can therefore permeate even dense clouds and dust.
Due to these advantages of neutrinos over "classical" astrophysical messenger particles neutrinos have been recognized as an essential new instrument to study astrophysical phenomena. Further information about the link between neutrinos and other messenger particles in the high-energy regime can be found in [11].

The small cross-section of neutrino interactions is also the main problem using these particles as messenger particles. Large detector volumes are needed to observe single neutrino events. Since the flux of neutrinos decreases with growing neutrino energy, even larger detector volumes are needed to search for the highest energy neutrinos. The currently largest neutrino detector, IceCube, has an instrumented volume of $1\,\mathrm{km}^3$ [1]. KM3Net, a neutrino detector

[1] In-ice Gain with Low-noise Unit, amplifier and signal converter in the ice
[2] Downhole Receiver and Amplifier Board, amplifier and signal converter on the surface

currently under construction in the Mediterranean Sea, will also have an instrumented volume of about 1 km^3 and will provide a complementary sky coverage to IceCube [3].
Both IceCube and KM3Net rely on Cherenkov radiation produced by high-energy secondary particles after a neutrino interaction in the detector medium. These particles propagate faster than the local speed of light and therefore produce Cherenkov light. This can be detected by optical receivers (photomultipliers).
In ice or seawater, which is used as a detector medium, the light is strongly attenuated after only a few meters. This would make it expensive to build even larger detectors, which would be needed to detect the low fluxes of the most energetic neutrinos.

In addition to Cherenkov light, there is another way to detect high-energy neutrino interactions: Radio radiation is produced by the formation and propagation of a particle shower after the interaction. This has a much longer attenuation length than optical light. Using this emission is the idea behind neutrino radio detection.

1.2. Neutrino radio detection

When a high-energy neutrino interacts with matter, it produces a large number of secondary particles, mostly photons, electrons, and positrons. This "swarm" of particles is commonly known as a particle shower. [19] Other types of high-energy particles, such as ultra-high-energy gamma photons or high-energy cosmic rays, also produce particle showers, but with different abundances of secondary particles.
There are two effects that cause a particle shower to produce radio emission: The first effect, called geomagnetic emission, is caused by the Earth's magnetic field and is predominant in air-propagating showers. The shower contains particles of different charges, such as positrons and electrons. These particles are affected by the Lorentz force as they move through the Earth's magnetic field. This leads to a linear charge separation, creating a dipole. This dipole moves with the shower, producing electromagnetic radiation.
The second effect is called Askaryan radiation, firstly described by G.A. Askaryan 1965 [6]. When a particle shower develops in a dielectric medium, the shower front can entrain electrons from the medium, leading to an excess of negative charge on the "bow wave". As a result, the shower resembles a dipole moving along the axis of propagation. This moving dipole produces coherent radio radiation. In a cone around the shower axis, under the so-called Cherenkov angle, the emission from the entire shower interferes constructively. As a result, the strength of the radio emission is most intense under this angle. [19] A sketch of the emission principle can be seen in Figure 1. The radio emission can be received by radio antennas in the medium, the signal ideally appears as a bipolar pulse.
A medium which is suitable for Askaryan radiation and available for free in large amounts is ice. It is transparent to radio emissions, with attenuation lengths of up to 2 km. Compared to optical attenuation lengths of up to 100 m, a more sparse instrumentation can be used. In addition, there is no need for kilometer-deep boreholes as required for optical detection. Small bubbles and dust, which are more abundant at lower depths, do not scatter radio waves as much as optical light. These points make radio detection a cost-effective method for studying the highest-energy neutrinos. [19]
For many years, the use of the Askaryan radiation to detect neutrinos or cosmic rays was only a theoretical consideration, but a publication in 2007 showed that the theoretical models for the generation of Askaryan radiation in ice were correct [9]. This was demonstrated by shooting

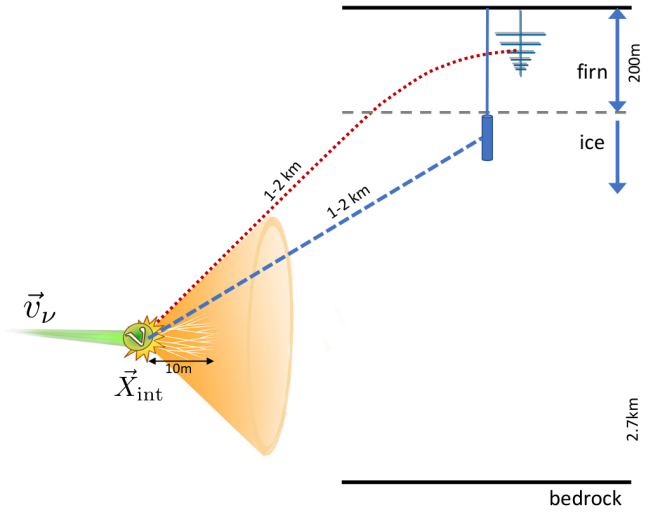

Figure 1: The principle of radio detection of neutrinos based on Askaryan radiation: After a high-energy neutrino interacts with ice, a shower of secondary particles is produced. During its propagation, this shower produces a cone of radio emission (the Askaryan radiation), which can be detected by antennas in the ice.[19]

particles from a particle accelerator at an ice target and measuring the radio emissions. This measurement was part of the ANITA (Antarctic Impulsive Transient Antenna) project.
ANITA was a balloon experiment to detect Askaryan radiation from high-energy neutrino interactions in the Antarctic ice shield. This experiment allowed monitoring of a neutrino detection volume of $1-2$ million cubic kilometers using antennas mounted on a stratospheric balloon floating above the Antarctic ice sheet. [4]
A ground-based radio neutrino observatory in Antarctica was ARIANNA (Antarctic Ross Ice-Shelf Antenna Neutrino Array) [7].
Another observatory, ARA (Askaryan Radio Array), is being built near the South Pole in Antarctica, next to the IceCube site [5]. IceCube-Gen2 will also include a radio array to improve sensitivity at neutrino energies beyond 30 PeV [10].
The Radio Neutrino Observatory in Greenland (RNO-G) is currently under construction in Greenland and is described in more detail in the next section.

1.3. RNO-G

The Radio Neutrino Observatory in Greenland (RNO-G) is a neutrino telescope under construction in Greenland. It relies exclusively on radio detection using Askaryan radiation produced by neutrino interactions in the Greenlandic ice sheet. Construction began in 2021 at Summit Station, the highest point on the Greenlandic ice sheet, at an altitude of 3200 m. RNO-G targets the neutrino energy range from 10 PeV to beyond 100 EeV. Since the Earth is opaque to neutrinos at these energies, RNO-G can only detect neutrinos from the Northern celestial hemisphere. [2]
Because of the large amounts of ice needed as detector material, only two areas can host such an observatory: Greenland and Antarctica. Greenland was chosen because it is more accessible than Antarctica. This is important because large amounts of material are needed during the installation phase. [2]

The design of the RNO-G observatory can be seen in Figure 2. In its final form, RNO-G will consist of a grid of 35 stations. Each station is connected to three strings of antennas, which are lowered into boreholes up to 100 m deep. Additionally, each station is connected to multiple "surface antennas". These antennas are Logarithmic Periodic Dipole Antennas (LPDA), installed directly below the ice surface. [2]

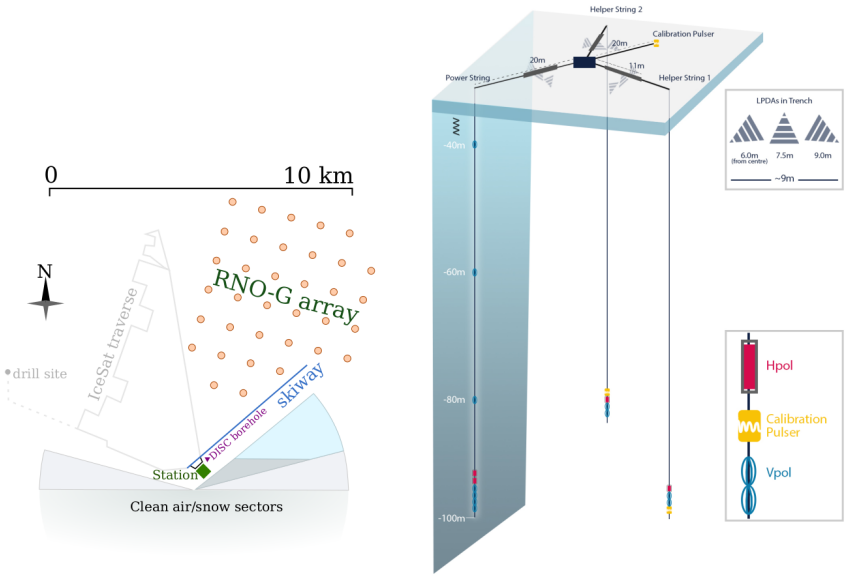

Figure 2: A schematic drawing of the RNO-G observatory. The observatory consists of 35 station with three instrumentation strings each. On the instrumentation strings are different types of antennas and calibration pulsers installed. Additional surface antennas are added to each station. [2]

This setup allows measuring the incident angle of the neutrino from the phase shift of the radio emission between the different antennas.
Due to a gradient in the refractive index from the upper firn layer to the old compact ice at greater depths, it is necessary to position the antennas deeper in the ice to prevent the radio waves from being refracted away from the antennas. [2] For this reason, the antennas have to be placed in boreholes in the ice.
The next section will now provide details on the RF components of the in-ice components.

2. Technical prerequisites

2.1. RNO-G Hardware

The instrument strings in the ice contain two types of antennas at different depths: Horizontal (Hpol) and Vertical (Vpol) polarized antennas. Vpol antennas are designed as dipole antennas, while the Hpol antennas are designed as less sensitive "Slot Antennas" due to the limited horizontal space in the boreholes [17].
The signals received by the antennas must be transmitted from the boreholes to the surface where they can be processed. Due to the long distance (antenna depth + surface cabling) between the antenna and receiver, a coaxial cable cannot be used. Such a long coaxial cable would introduce additional noise and attenuation and would have inappropriate spectral

transmission characteristics. [17] Instead, a method commonly used in radio astronomy and telecommunications was adopted.
This method, called RFoF (RF over fiber), works in the following way: The signal is transmitted through a short coaxial cable to a preamplifier in the hole. The amplified signal drives a laser diode, which emits the RF signal as an infrared light signal through a long optical fiber. At the surface, the light signal is received by a photodiode that drives another amplifier. This amplifier outputs the RF signal that travels through short coaxial cables to the data acquisition system. This is a simplified description since both the in-ice and surface modules contain additional filtering and impedance matching circuitry. The total gain of the IGLU-DRAB chain is designed to be greater than 60 dB. [17]
The in-hole module that amplifies the antenna signal and converts it to optical signals is called IGLU (In-ice Gain with Low-noise Unit). The module that converts the signals to electrical signals and further amplifies them is called DRAB (Downhole Receiver and Amplifier Board) [17]. A DRAB board has four channels, i.e. a DRAB board allows the simultaneous connection of up to four IGLU boards / antennas. An IGLU board is connected to only one antenna. A block circuit diagram of one channel of an IGLU-fiber-DRAB chain can be seen in Figure 4. A picture of an assembled IGLU and DRAB board can be seen in Figure 3.

Figure 3: A DRAB module (left) and a IGLU module (right). Together with a connecting fiber optic cable, these two modules form the IGLU-fiber-DRAB chain.

The RF connectors on both modules are coaxial SMA connectors with 50 Ohm impedance. The DRAB board is also powered from an SMA connector. The IGLU board has two N-type connectors that allow the supply voltage to be looped through, therefore only one supply line is required in the borehole. The typical supply voltage is $3.3 - 3.5\,\mathrm{V}$. On the IGLU side, the fiber is connected with a so-called FC/APC simplex fiber adapter, on the DRAB board, the fiber is connected with an SC/APC connector [17]. While the FC connector is secured with a union nut when connected, the SC is a click connector that allows easier reconnection.

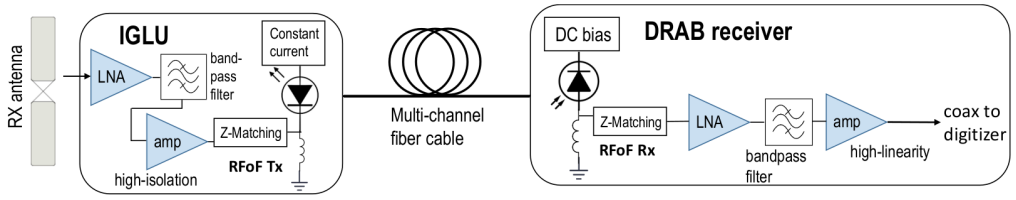

Figure 4: Block circuit diagram of one channel of a IGLU-fiber-DRAB chain (RFoF). [17]

After passing through the IGLU-fiber-DRAB chain, the signal is routed to the RADIANT board (Radio Digitizer and Auxiliary Neutrino Trigger) where it is digitized and various event trigger mechanisms are applied to the signal. Captured Events are sent via LoRa communication wirelessly to the Summit Station. Here the data is stored on hard drives. [2]

2.2. S-Parameters of RF-Devices

An important parameter for describing a radio frequency (RF) device is its impedance Z, which is the complex extension of electrical resistance. Like resistance, it describes the relationship between voltage and current, but it also takes into account the phase shift between these values. Voltage and current in RF circuits are usually assumed to be waves. The formula for power is the same as for DC: $P = \frac{U^2}{Z}$

When the impedance of the current path changes at a point in the circuit, the wave is completely or partially reflected. The optical analog is the reflection of light at the interface of two media with different refractive indices.

Due to this reflection, the following applies to the transported power in the forward direction at point x in the circuit [18]:

$$P(x) = P_{\text{forward}}(x) - P_{\text{backward}}(x) = \frac{U_{\text{forward}}(x)^2}{Z} - \frac{U_{\text{backward}}(x)^2}{Z} \tag{1}$$

Here U_{forward} and U_{backward} are the momentary voltages of the forward and backward propagating waves.
From this equation we can define the Normalized Wave Amplitude, which is the voltage normalized by the square root of the impedance:
The Normalized Wave Amplitude of the forward going wave [18]:

$$a(x) = \frac{U_{\text{forward}}(x)}{\sqrt{Z}} \tag{2}$$

The Normalized Wave Amplitude of the backwards going wave [18]:

$$b(x) = \frac{U_{\text{backward}}(x)}{\sqrt{Z}} \tag{3}$$

This scheme is now applied to the input (Port 1) and output (Port 2) of an RF device. a_x is the amplitude of the ingoing signal at the respective port, b_x is the amplitude of the outgoing

signal at the respective port. This makes it possible to construct a so-called Scatter Matrix for this device (which is now called network), which relates the incoming and outgoing signal amplitudes to each other [18]:

$$\begin{pmatrix} b_1 \\ b_2 \end{pmatrix} = \underbrace{\begin{pmatrix} S_{11} & S_{12} \\ S_{21} & S_{22} \end{pmatrix}}_{\text{Scatter Matrix}} \cdot \begin{pmatrix} a_1 \\ a_2 \end{pmatrix} \tag{4}$$

The entries of the Scatter Matrix S_{xy} are called S-parameters. Here x is the port where the wave is outgoing and y is the port where the wave is ingoing. They are dimensionless and complex values, since each S-parameter represents the amplitude and phase relationship of the in- and outgoing waves. These S-parameters are typically frequency dependent. An RF device with N inputs has N^2 S-parameters, which are arranged in an $N \times N$ matrix. [18] In this work, only RF devices with two ports are considered.
The individual S-parameters have the following meaning [20]:

- $S_{11} = \frac{b_1}{a_1}|_{a_2=0}$ Reflected wave at Port 1, when no incoming wave at Port 2
- $S_{22} = \frac{b_2}{a_2}|_{a_1=0}$ Reflected wave at Port 2, when no incoming wave at Port 1
- $S_{21} = \frac{b_2}{a_1}|_{a_2=0}$ Transmission of a wave from port 1 to Port 2, when no incoming wave at Port 2
- $S_{11} = \frac{b_1}{a_2}|_{a_1=0}$ Transmission of a wave from port 2 to Port 1, when no incoming wave at Port 2

The S-parameters are usually specified in dB. Due to the corresponding definition of dB, the values therefore apply to both voltage and power ratios. If the S-parameters are specified as linear magnitudes, this value refers to the voltage ratios.
S-parameters are typically measured using a VNA (Vector Network Analyzer). The working and operation principle will be explained in the next section.

2.3. Basics of a Vector Network Analyzer

A Vector Network Analyzer is a measuring device with one, two or more ports. These ports are connected to the inputs and outputs of the device under test (DUT). Each port can transmit an RF signal (stimulus signal) and measure the response of the DUT on that port (reflection) and on the other ports (transmission). The stimulus signal typically sweeps from an adjustable minimum frequency to an adjustable maximum frequency. [20] The response of the DUT is analyzed at an adjustable number of points. This number determines the spectral resolution of the measurement. In addition, an adjustable number of sweeps can be averaged for noise suppression.
There are three components behind each port of the VNA: an RF source, a receiver with preamplifier and a "direction isolator", which should be a so-called circulator, which routes the signals from the RF source to the port, and the incoming signals to the receiver. This allows the simultaneous transmission of the stimulus and reception of the reflection. The output power transmitted from the VNA port into the DUT can be adjusted for each port. Also, the gain of the preamplifier can be set for each port. With the VNA used in the following, there

were only the settings “High” and “Low”. The gain of the receiver could be set for each port, depending on the sending port. The gain should be set as high as possible in order to avoid additional noise during the digitization of the signal (digitization noise). But, saturation due to excessive gain of the receiver must be prevented.
Due to the ability to send and receive signals simultaneously at each port, a VNA is predestined to measure S-parameters. It is also possible to measure the propagation delay of the signal (group delay) through the DUT. Both the ratio of the reflected/transmitted signals and their phase shift can be measured [20]. Which measurements are carried out can be set in the measurement application on the controlling computer. The controlling application is typically provided by the manufacturer of the VNA.
The VNA is factory calibrated, but this calibration only covers the internal components up to the port connectors. However, the cables and connectors between the VNA and DUT can distort the measured values, making it necessary to calibrate the measurement setup. [20] This can be done in two ways:

Manual calibration

Manual calibration is a step-by-step routine. All connectors to be connected to the DUT must be measured open, short-circuited and terminated with matching impedance. A “through” measurement is also performed, in which two connectors are connected directly to each other. During these steps, the measurement application collects all the parameters needed to correct the measured values. [20] The calibration measurements are made using a manual calibration kit, as shown in Figure 5.

Figure 5: A manual calibration kit provides several types of line terminations required during manual calibration. [20]

ECAL

A ECAL (electronic calibration) makes a VNA calibration fully automatic. The ECAL device is connected instead of the DUT to the VNA and performs all needed steps automatic. Directly controlled by the measurement application via USB, it allows a easy and fast calibration of the VNA. [20]
The values determined during the actual measurement are corrected using the values determined during calibration. The equations used for correction can be found here: [12].

3. Experimental Setup

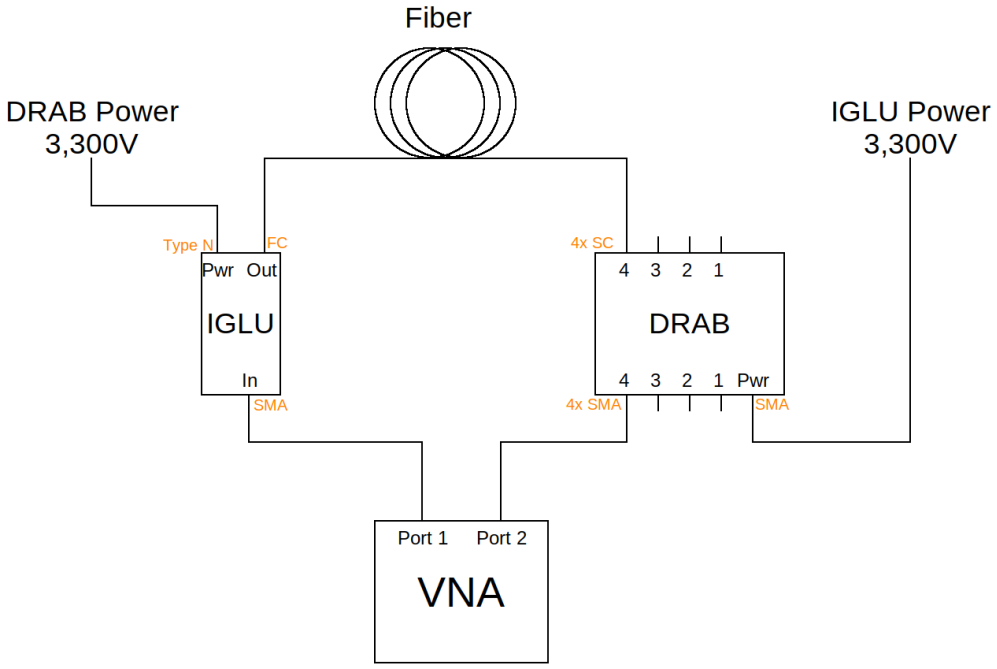

Figure 6: A schematic drawing of the measurement setup. The orange annotations at the connectors label the connector type.

In order to properly model the RNO-G hardware, several parameters of the IGLU-Fiber-DRAB chain has to be determined. The following parameters can be measured using a VNA:

- Transmission Gain, the S_{21} parameter and it's phase. Hereinafter referred to as "gain".
- Reflection on the IGLU input, the S_{11} parameter and it's phase.
- Reflection on the DRAB output, the S_{22} parameter and it's phase.
- Reverse Isolation, the S_{12} parameter and it's phase.
- Group Delay of signals transmitted through the IGLU-Fiber-DRAB chain.

A schematic of the setup to measure the S-parameters of the individual DRAB boards is shown in Figure 6. To measure the S-parameters a Keysight P5020A was used in two port configuration. The setup consists of the VNA, whose port 1 is connected to the antenna input of the IGLU board. The "Reference IGLU" (`Amp_IGLU_C1000`) was commonly used for all following measurements. The output is connected via a FC fiber connector, to a fiber. The 50 m long "Reference Fiber" was used unless otherwise stated. The other terminal of the fiber, a SC fiber connector, is plugged in a input of a DRAB board. Here the "Reference DRAB" (`Amp_DRAB_C0038`) was used mainly. The output of the DRAB board was connected to Port 2 of the VNA.
Both, the IGLU and DRAB board is powered by a two channel adjustable power supply. A voltage $U_{\mathrm{IGLU}} = U_{\mathrm{DRAB}} = 3.300\,\mathrm{V}$ was used, unless otherwise noted.

According to the manufacturer's instructions, the VNA must warm up for 60 minutes before starting a series of measurements[13]. This requirement was met in all measurements.
Before starting measuring the S-Parameters the VNA needs to be calibrated. This needs to be done mainly due to the fact that the connectors and cables between the VNA and the DUT (in this case the IGLU-Fiber-DRAB chain) change the S-parameters slightly. For all calibrations a ECAL was used. More details about the calibration process can be found in subsection 4.2.
The VNA is controlled by a GUI-Application on a computer. The measurement data itself is retrieved from this application via a Python script based on pyVISA. An example of such a python script is shown in subsection A.2. A modified version of this script was used for all subsequent measurements.
Before optimizing the calibration, the following settings were used for measurement and calibration:

- Frequency Range: $1\,\text{MHz} - 1\,\text{GHz}$
- Frequency Resolution: $2001\,\text{Points} \approx 0.499\,\text{MHz}$
- Port 1 Power: $P_{\text{Port1}} = -60\,\text{dBm}$
- Port 2 Power: $P_{\text{Port2}} = -60\,\text{dBm}$
- Averaging: 100 Sweeps

4. Experiment and Evaluation

4.1. First Measurements

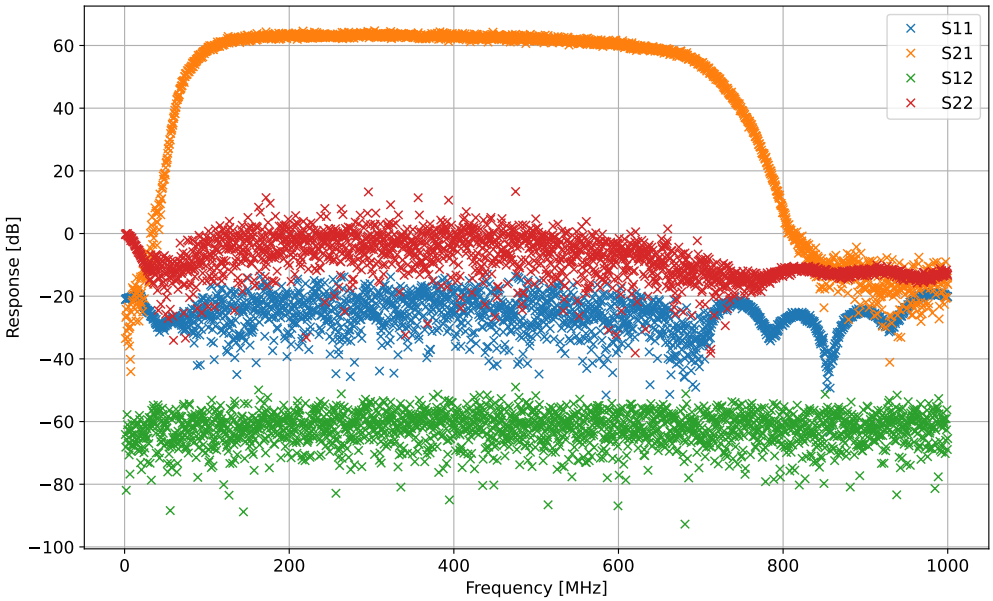

Figure 7: The first measurements of the S_{xy} parameters showed significant noise and strange behavior of the reflection parameters.

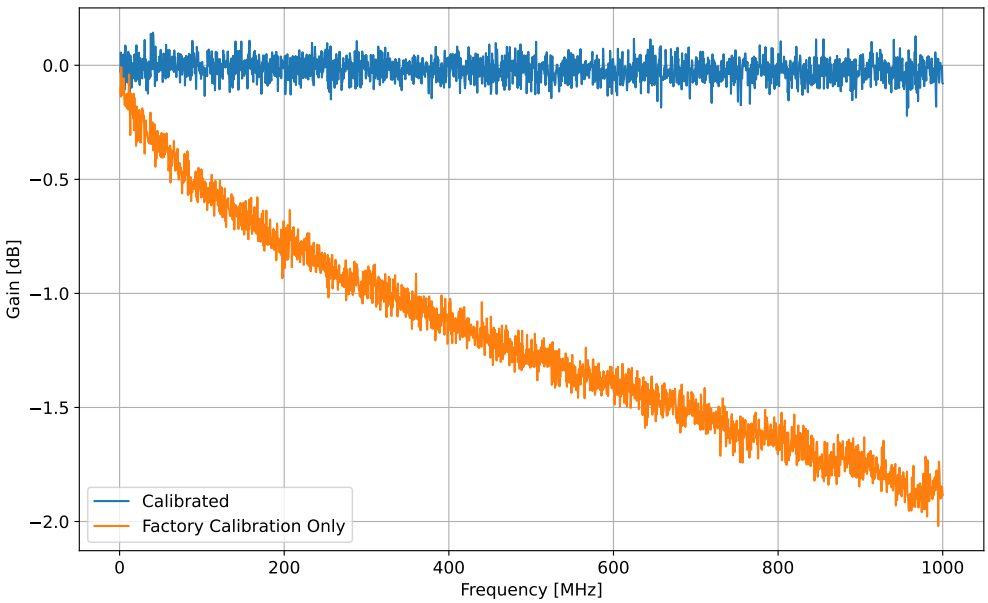

Figure 8: A comparison between two "Through" measurements, one calibrated using ECAL and one only using the VNA factory calibration.

In Figure 7 one of the first measurements is shown. The first measurements showed a strange behavior of the reflection parameters, especially S_{22}: The parameter was measured $> 0\,\mathrm{dB}$. This is non-physical due to energy conservation and was a first indication of a problem in the VNA calibration. As described in subsection 2.3 the outputted data is not directly measured, it is internally calculated from the measured data and the data collected during calibration. In the RNO-G hardware calibration measurements so far, this issue was mitigated by putting a 20 dB attenuator between the DRAB output and the VNA port. This additional attenuation was calculated out by leaving the attenuator at Port 2 of the VNA during calibration of the VNA.
Furthermore, the measured data showed significant noise. For the reflection parameter, the previous issue seems to be a result of this. The first idea to tackle the high noise is to increase the number of averages per measurement, but the noise stayed at a high level. The noise seemed to converge to a fixed pattern of noise. Without applying the calibration to the measurement, the noise was reduced significantly. However, calibration must not remain deactivated for a proper measurement of the parameters. A comparison between an uncalibrated and a calibrated "Through" measurement can be found in Figure 8. "Through" means that a simple connection of both cables to the VNA ports has been set instead of connecting the DUT to the circuit. On the uncalibrated measurement only the internal factory calibration was applied. According to this measurement the part of the circuit which is not included in the factory calibration (cables and connectors), shows a pronounced low-pass behavior. Therefore, a way must be found to reduce the noise even with using the calibration.

4.2. VNA-Calibration and Optimization

One way to reduce the noise in the calibration (and also in the measurement) is to increase the output power of the VNA ports. This would increase the SNR, since the inherent noise of the amplifiers in the VNA, as well as external noise sources stay constant, while the signal am-

plitude increases. However, it is not possible to increase the output power of the ports of the VNA to values much higher than −60 dBm, as this would lead to saturation of the amplifiers in the IGLU- and DRAB-Boards. In order to still use higher output power at the VNA ports, various combinations of attenuators were tried. This led to another problem during calibration: When trying to calibrate the system with the attenuators, the automatic connection detection failed often. This happens at the beginning of the calibration, when the system checks which VNA port is connected to which port of the ECAL device. A solution of this would be using a manual calibration of the VNA. But this and the fact that additional components are added to the circuit, increases the complexity of the measurement and therefore the probability of errors.

The manufacturer of the VNA recommends, when measuring high gain systems, another way [14]: The output powers of the two VNA ports should be set to "uncoupled" in the VNA application. This allows to increase only the output power of Port 2, which is only connected to the output of the DRAB-Board. Therefore, there is no risk of saturating one of the amplifiers in the DRAB or IGLU, but it is possible to measure the S_{22} and S_{12} parameter with higher SNR. This should also lower the noise introduced by the calibration, since the calibration depends on measuring these parameters. Therefore, it influences the noise of the measurement result through error propagation when calculating the outputted data. The output power of Port 2 was increased to $P_{\text{Port2}} = -10\,\text{dBm}$, while Port 1 stays at $P_{\text{Port2}} = -60\,\text{dBm}$.
However, this only resulted in a slight reduction in noise.

An additional step, made it possible to significantly reduce the noise: Increasing the output power during the calibration and resetting it lower power during measurement.

To get a higher SNR during calibration the output power of Port 1 of the VNA was increased to $P_{\text{Port1}} = -30\,\text{dBm}$, Port 2 was operated at $P_{\text{Port2}} = -10\,\text{dBm}$. After calibration the power of Port 1 was re-set to $P_{\text{Port1}} = -60\,\text{dBm}$.

If the output power of Port 1 would be increased to more than $P_{\text{Port1}} = -30\,\text{dBm}$, the VNA refuse to use the calibration for the measurement at $P_{\text{Port1}} = -60\,\text{dBm}$, while a lower power during calibration would decrease the SNR. This is why $P_{\text{Port1}} = -30\,\text{dBm}$ is the optimal value to be used during calibration.

When using $P_{\text{Port1}} = -30\,\text{dBm}$ during calibration, it is important to set the receiver gain in direction Port 2 →Port 1 to "Low". Otherwise, the VNA receiver at Port 1 would saturate due to the high output power at Port 2 during the "through" calibration step This value should be re-set to "High" after calibration, to reduce digitization noise during measurement.
For further noise reduction, the averaging was increased from 100 Sweeps to 300 Sweeps. The downside of this step is that the time per measurement increases from $\approx 17\,\text{s}$ to $\approx 51\,\text{s}$.

A comparison of S_{21} measurements using different calibration settings can be seen in Figure 9. For the DUT the "Through" path of a manual VNA calibration kit was used, thus the cables to the VNA ports where simply connected together. Therefore, a frequency-independent S_{21} of 0 dB is expected. The legend labels of the plot have the following format: P_{Port1} during calibration / P_{Port2} during calibration / N_{avgs} Number of averaged sweeps during calibration. During measurement always the following settings were applied: $P_{\text{Port1}} = -60\,\text{dBm}$, $P_{\text{Port2}} = -10\,\text{dBm}$ and averaging $N_{\text{avgs}} = 500$ sweeps.

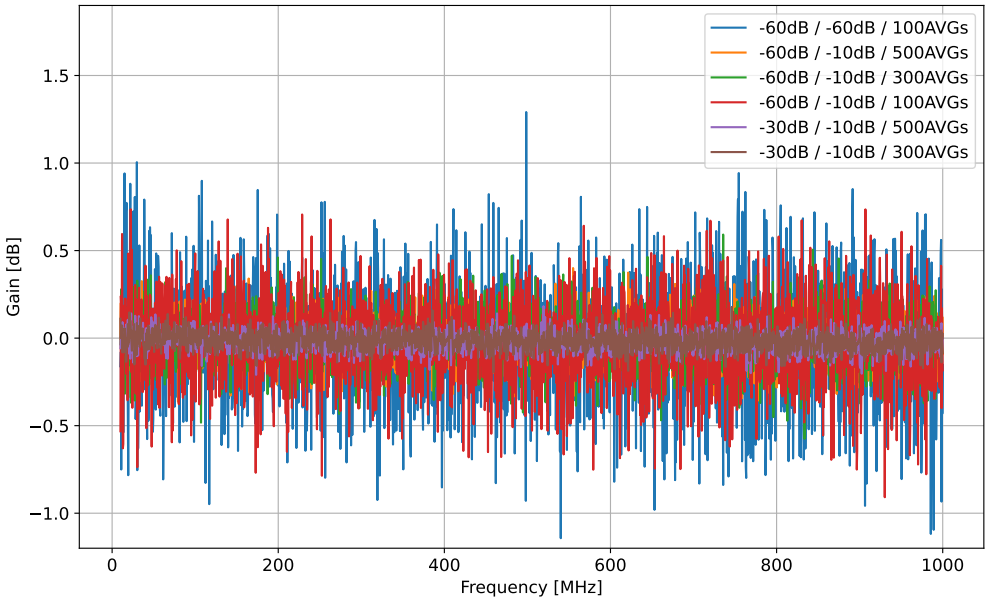

Figure 9: A comparison between different calibration settings. DUT was the through path of a manual VNA calibration kit. The format of the legend labels are explained in the text.

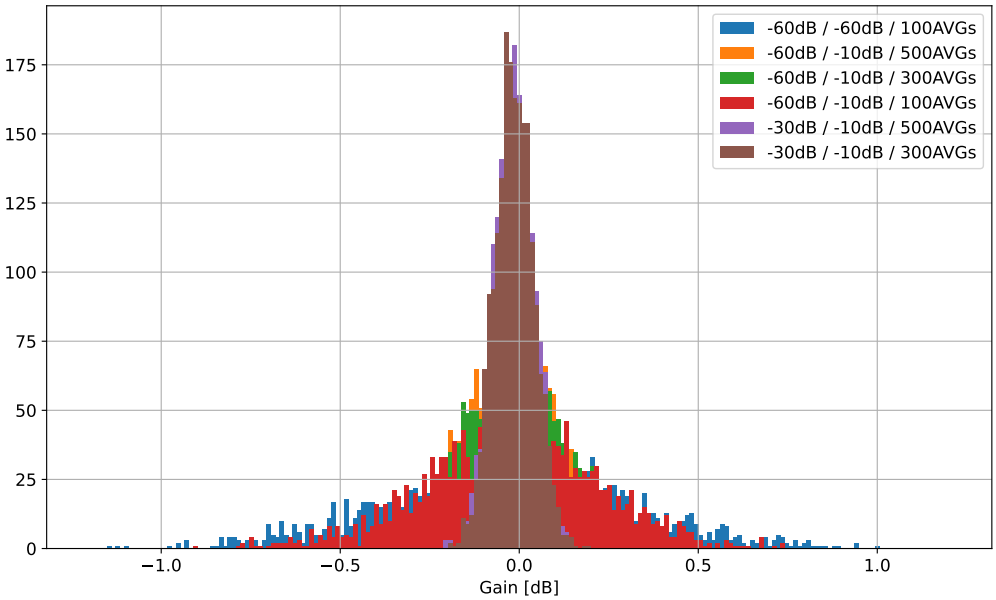

Figure 10: Histogram of the values measured using different calibration settings. DUT was the through path of a manual VNA calibration kit. The format of the legend labels are explained in the text.

For a better comparison the distribution of the measured gains are displayed as a histogram in Figure 10. The following statistical values could be obtained by calculating the average (S_{21} AVG) and the standard deviation (S_{21} Std. Dev.) of the S_{21} parameters over the entire measured frequency range (1 MHz – 1 GHz):

P_{Port1} [dBm]	P_{Port2} [dBm]	N_{avgs} [sweeps]	S_{21} AVG [dB]	S_{21} Std. Dev. [dB]
−60	−60	100	−0.03	0.33
−60	−10	100	−0.02	0.24
−60	−10	300	−0.02	0.15
−60	−10	500	−0.02	0.12
−30	−10	300	−0.01	0.06
−30	−10	500	−0.02	0.05

The stepwise improvement of the measured data can be seen from this data. The first reduction of the noise was done by uncoupling the power of the output and setting $P_{\text{Port2}} = -10\,\text{dBm}$. The second improvement was increasing of output power on Port 1 to $P_{\text{Port1}} = -30\,\text{dBm}$. Finally, a slight improvement was done by increasing the number of averages.
After all improvements a noise level of 0.06 dB could be achieved. This is in the same magnitude as the measuring accuracy specified by the manufacturer for the range $50\,\text{MHz} - 3\,\text{GHz}$ (see Figure 11). In this range the manufacturer specifies an accuracy of $\approx 0.04\,\text{dB}$ for a VNA of the same series as used [13]. Further improvement of the measurement accuracy is therefore hardly possible, as this would be limited by the (systematic) measurement inaccuracy

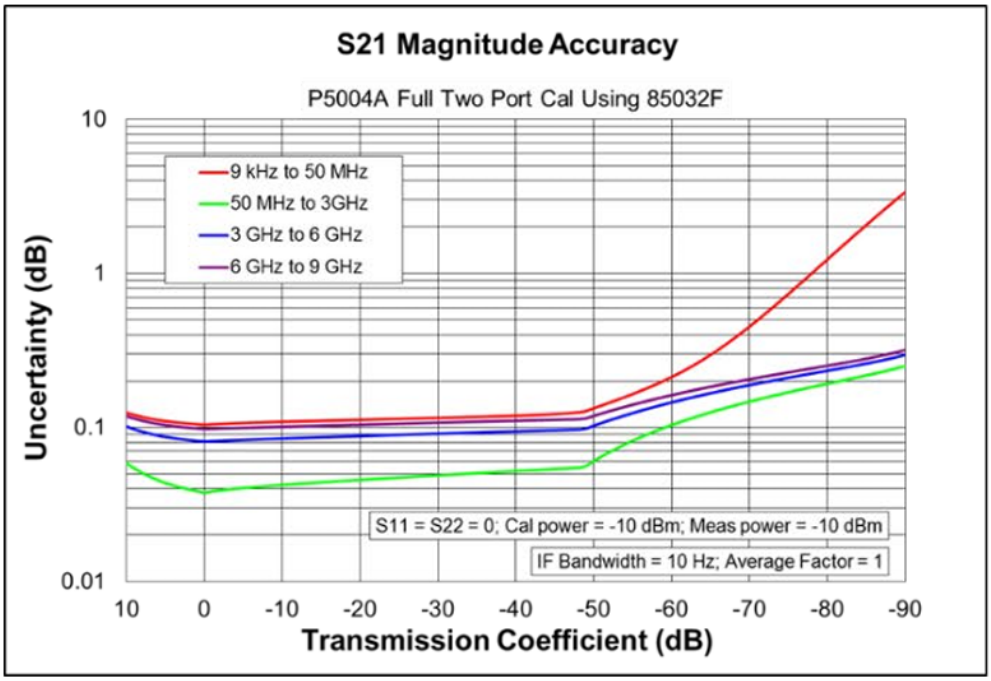

Figure 11: The accuracy of S_{21} measurements according to the manufacturer [13]. To compare this to the "Through" measurement, the value at a Transmission Coefficient of 0 dB is relevant.

Step-by-step instructions to calibrate the VNA can be found in subsection A.1.
A plot showing the reduction of noise in an IGLU-fiber-DRAB-chain measurement is shown in Figure 12.

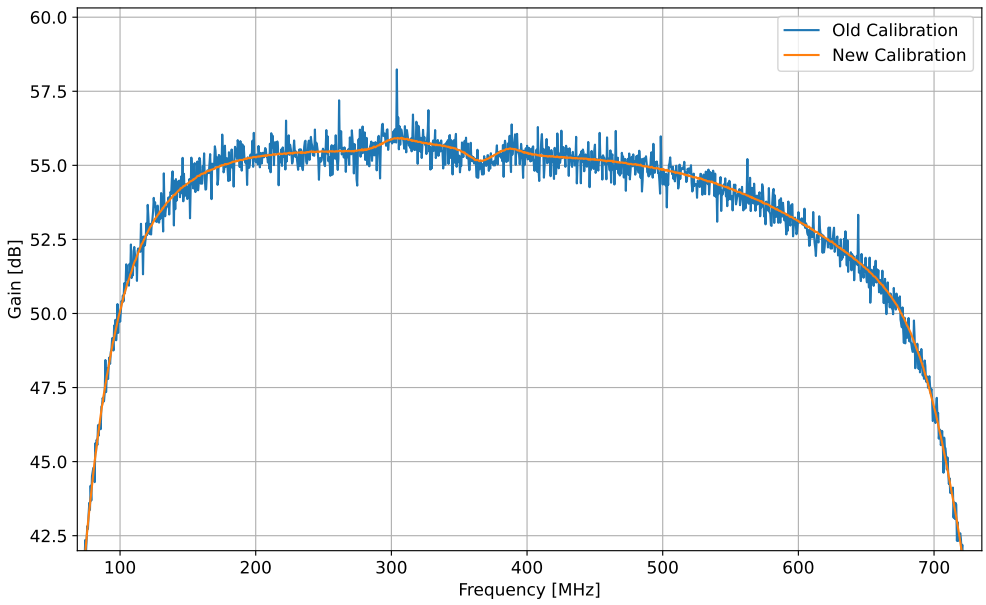

Figure 12: Also when measuring the IGLU-DRAB chain the noise could be reduced significantly.

4.3. Influence of the connectors

After improving the calibration of the VNA, precise measurements for the reproducibility of the measurement results can now be started. Even before this work was started, it was known that the S_{21} measurement results, after unplugging and reconnecting the fiber connectors, differed slightly. To quantify this behavior a linear fit was used, which was applied to the measurement data at a suitable frequency range. The linear fit function is of the form:

$$S = m \cdot (f - f_0) + S_0 \tag{5}$$

Here is S the S_{21} parameter at frequency f. f_0 is the frequency where the S_{21} parameter offset S_0 is evaluated. m is the fitted slope of the S_{21} parameter in the range used.
A suitable frequency range has turned out to be $460 - 550\,\mathrm{MHz}$, while $f_0 = 500\,\mathrm{MHz}$ has been used. A fit on this frequency range on measured data can be seen in Figure 13. Due to many "features" on the S_{21} data only a small range is suited for a linear fit. The features may originate from different cut-off frequencies and resonances of the components on the IGLU/DRAB boards.

Now is it possible to quantify existing fluctuations between the measurements, the reproducibility of the measurement when unplugging and reconnecting the fiber can be checked. For this purpose, 100 measurements were carried out, between which the fiber connection was disconnected and reconnected (Hereafter commonly referred to as "broken"). This reconnection has been done at the SC connector on the DRAB side of the fiber. Similarly, 100 measurements were carried out between which no disconnection took place (Hereafter commonly referred to as "fixed"). These two measurement series can now be compared by doing a linear fit on each single measurement. The results can be seen in Figure 14. The plotted errors are the estimated fit errors of the scipy curve fit algorithm.

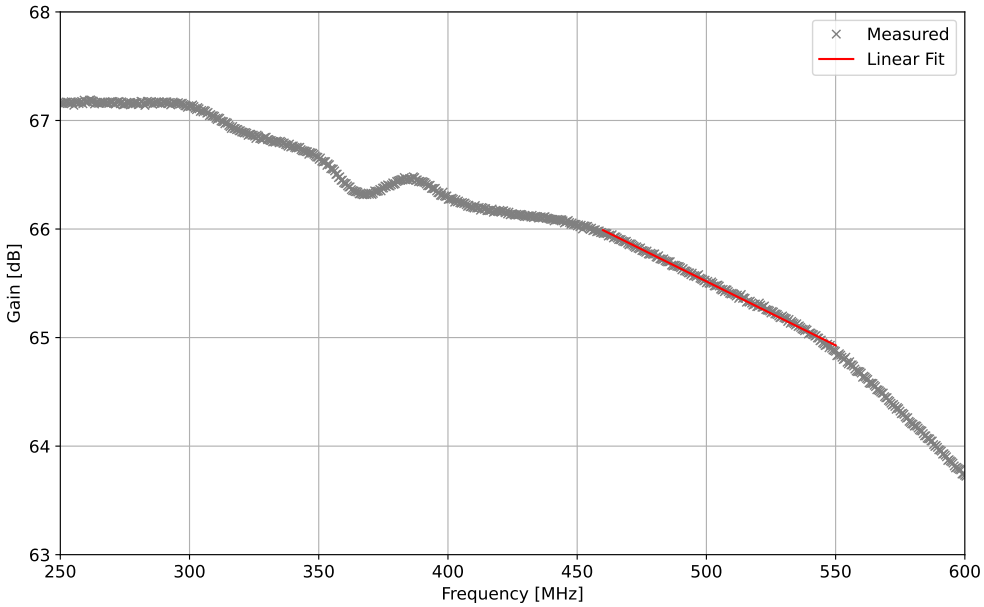

Figure 13: A linear fit on the measured S_{21} parameter in the frequency range $460 - 550\,\mathrm{MHz}$.

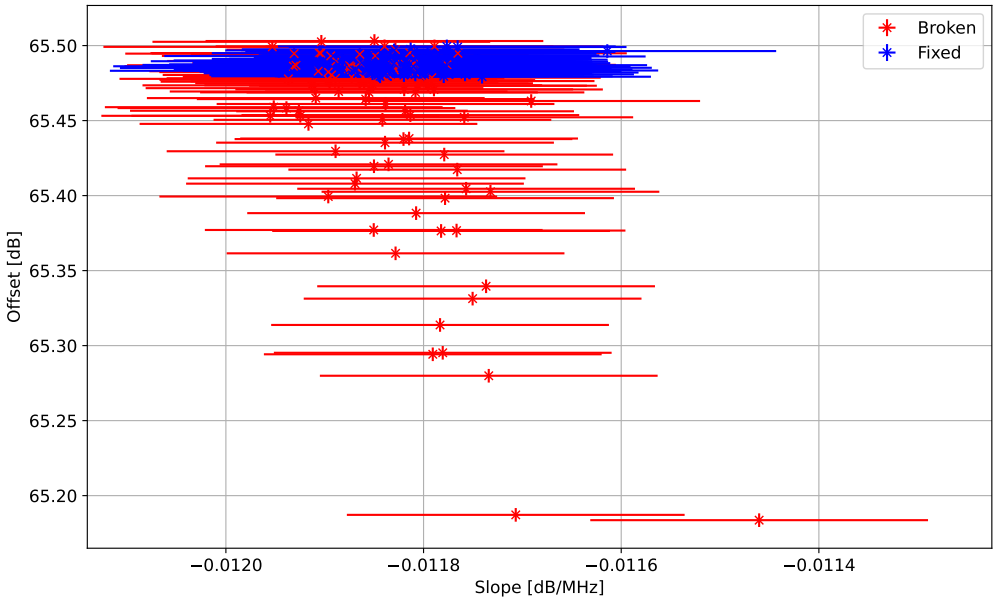

Figure 14: Parameters of linear fits on 100 "fixed" (no reconnection between measurements) and 100 "broken" (reconnected fiber between measurements) measurements.

The scatter of the slope can be explained by noise, since the estimated error is larger than the measured scatter. The offset scatter of the "broken" measurements is significantly higher than in the "fixed" measurements. In numbers: The standard deviation of the offset in the "broken" measurements is 0.10 dB and for the "fixed" the standard deviation is 0.005 dB. With the scattering of the "fixed" values, it can be assumed that it is only due to noise, but the significantly increased scattering of the "broken" values indicates that the reconnection leads to an actual change in the transfer function of the IGLU-DRAB chain.

The hypothesis that emerges is that this may be associated with the SC connectors on the DRAB. To validate this theory another measurement has been done: The plug was pressed in each direction in order to see whether this had an influence on the measured S_{21} parameter. In each direction 5 measurements were done. The directions are labeled as seen in Figure 15, the arrows indicate the direction in which the cable end of the plug was pressed.

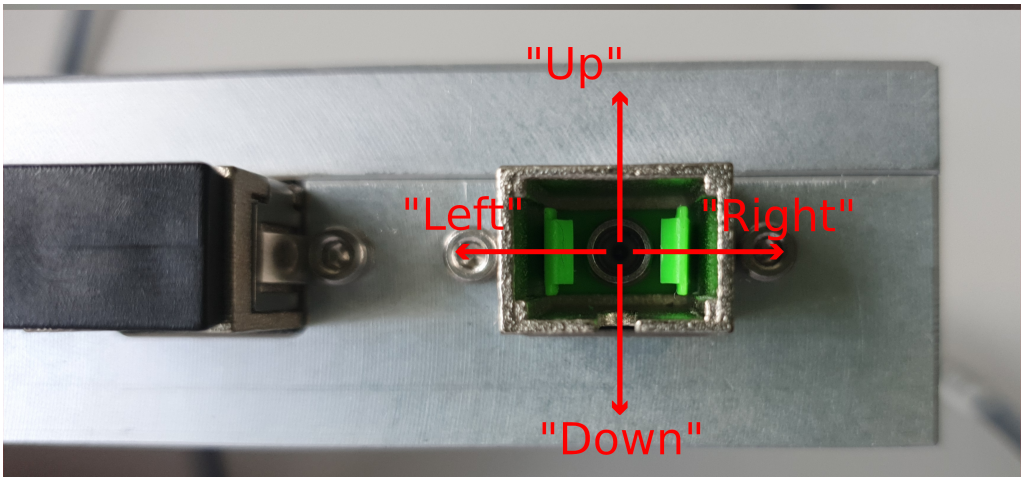

Figure 15: Directions of pressing (at the plug end) during the measurement of the influence of the SC plug on the S_{21} parameter

Similar to the previous measurement, a linear fit has been used to quantify the deviations. The same fit range and f_0 has been used as in the measurement series before. The results can be seen in Figure 16.

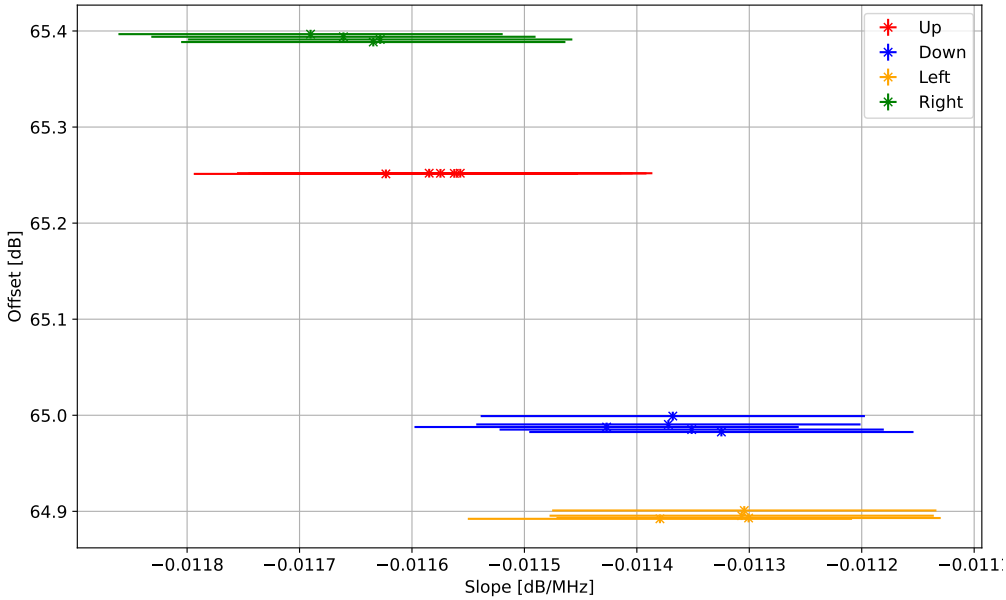

Figure 16: The gain of the IGLU-DRAB chain is influenced by the direction in which the SC plug is pressed.

This measurement showed a strong dependence between the pressed direction of the plug and the S_{21} parameter. This behavior does fully explain the scatter of the “broken” measurement

series. The maximum difference in gain that occurred in this series of measurements is 0.515 ± 0.006 dB. The standard deviation is 0.20 dB, which is in the same magnitude as in the "broken" measurement series (0.10 dB).
The gain variation can therefore be explained by the fact that there is a slight deviation in the alignment of the plug due to reinsertion or lateral forces. This change in orientation is likely to change the properties of the optical interfaces between the fiber and the photo diode. For example by changing the reflection/transmission ratio, which cause a change in the transmission properties though the complete chain.
Now that the phenomenon is known for the SC connector on the fiber, the FC connector at the IGLU side of the fiber was also examined for dependence on lateral forces. Here too, the plug was pressed in each direction. The directional designations for the cable end of the plug are as follows: "Right" - in direction to the power connector, "Left" - away from the power connector, "Up"/"Down" - corresponding to an IGLU with lid facing upwards. The SC connector on the DRAB side was untouched during this measurement series.

The fit parameter, using the same fit range as in previous measurement, are plotted in Figure 17.

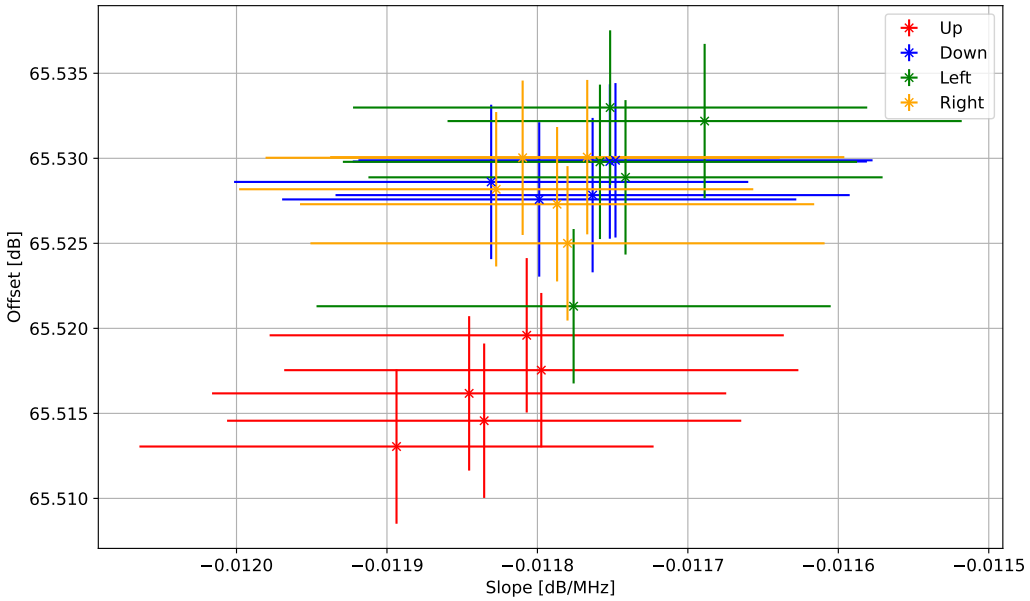

Figure 17: Lateral forces on the FC plug on the IGLU side of the fiber seem to have no influence on the gain of the IGLU-DRAB chain.

As can be seen in this plot, the variations in the gain are marginally greater than the errors in the fit parameters. A slight systematic deviation can possibly only be recognized in the "Up" direction, but this hardly goes beyond the variations between the measurements. It can therefore be assumed that these connectors achieve significantly more reproducible results when reconnecting than the SC connectors. This is likely due to the design of the plugs, as the carrier of the end of the fiber in this type of plug is inserted into a fitting on the socket side. The entire connection is secured with a union nut. This makes it nearly impossible for the optical interfaces to tilt against each other and should therefore prevent a change in the reflection/transmission properties.

In summary, it can be said that it would be better to use FC connectors at both ends of the fibers to ensure the reproducibility of the measurements.

4.4. Influence of power voltage variations

After analyzing the influences of the connectors, now the influence of the supply voltage on the gain of the IGLU an DRAB boards will be analyzed. At all previous measurements, the supply voltage was $U_{\mathrm{IGLU}} = U_{\mathrm{DRAB}} = 3.300\,\mathrm{V}$. The supply voltage is internally reduced by Low Dropout Voltage Regulator (LDO) to 2.7 V for the DRAB board [15] and 2.5 V for the IGLU board [16].
The internal LDOs should keep the internal voltage, which influences the gain, almost constant even when the supply voltage changes. Therefore, no strong changes are expected when changing the supply voltage, except when reducing it under the minimum required voltage of the LDOs. According to the schematics the minimal voltage for the DRAB is 3.1 V [15].
To measure the dependence on the supply voltage of the IGLU, its supply voltage is varied in a range from 2.0 V to 5.0 V volts while it is kept constant at 3.3 V on the DRAB board. On the measured S_{21} parameter, again the linear fitting has been done. The offset fit parameter versus supply voltage can be seen in Figure 18.

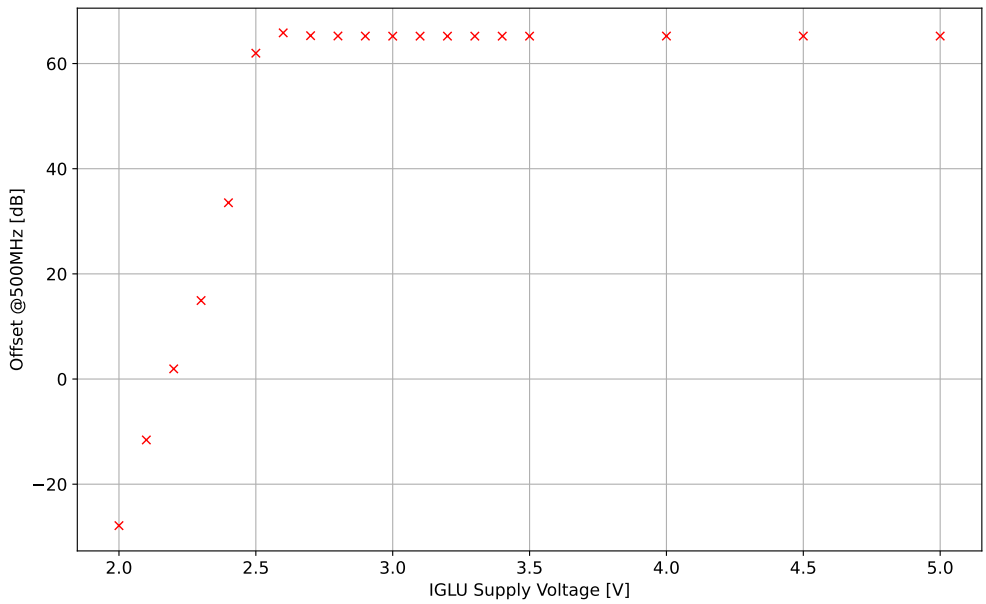

Figure 18: The offset of the linear fit at a frequency of 500 MHz versus the supply voltage of the IGLU board.

From this plot it is visible that the minimal voltage which does not affect the gain is $\approx 2.8\,\mathrm{V}$. Above this voltage the gain is constant. By zooming into this area (see Figure 19), only variations of 0.03 dB are visible, this is as low as the noise floor of the VNA.
The same procedure is being used for the DRAB board. Here the supply voltage is varied in a range from 2.0 V to 5.0 V volts while for the IGLU board the supply voltage is kept constant at 3.3 V. Also, here on each measurement a linear fit has been done and the offset parameter at 500 MHz has been plotted over the supply voltage (see Figure 20). Here the gain drops if

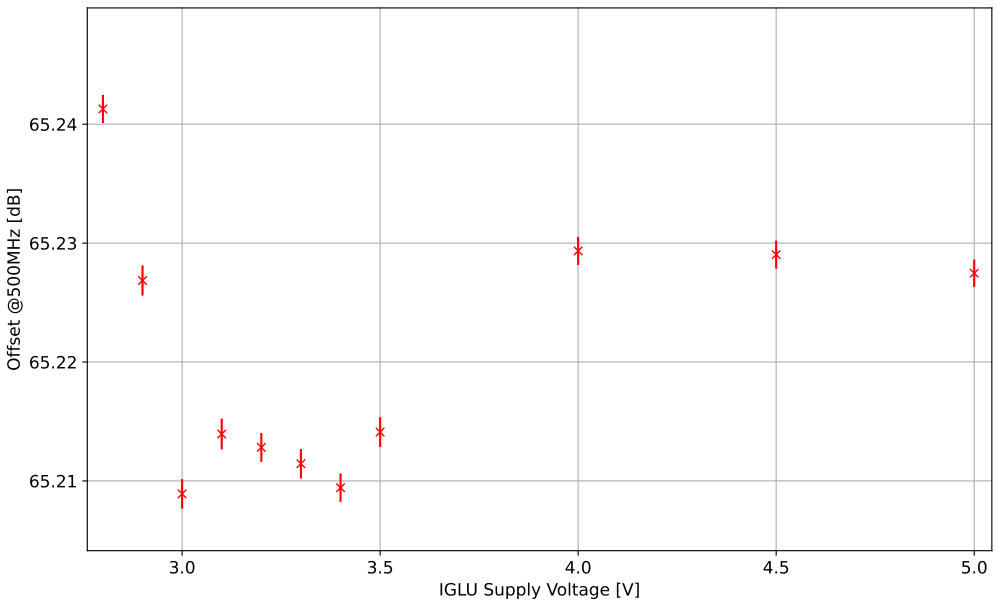

Figure 19: The offset of the linear fit at a frequency of 500 MHz versus the supply voltage of the IGLU board. Zoomed into the stable range above 2.8 V

the supply voltage is below 3.0 V. For $U_{\mathrm{DRAB}} > 3.3\,\mathrm{V}$ the gain is constant. The variations are smaller than 0.02 dB, that is even smaller than the expected measurement accuracy (see zoomed plot in Figure 21).

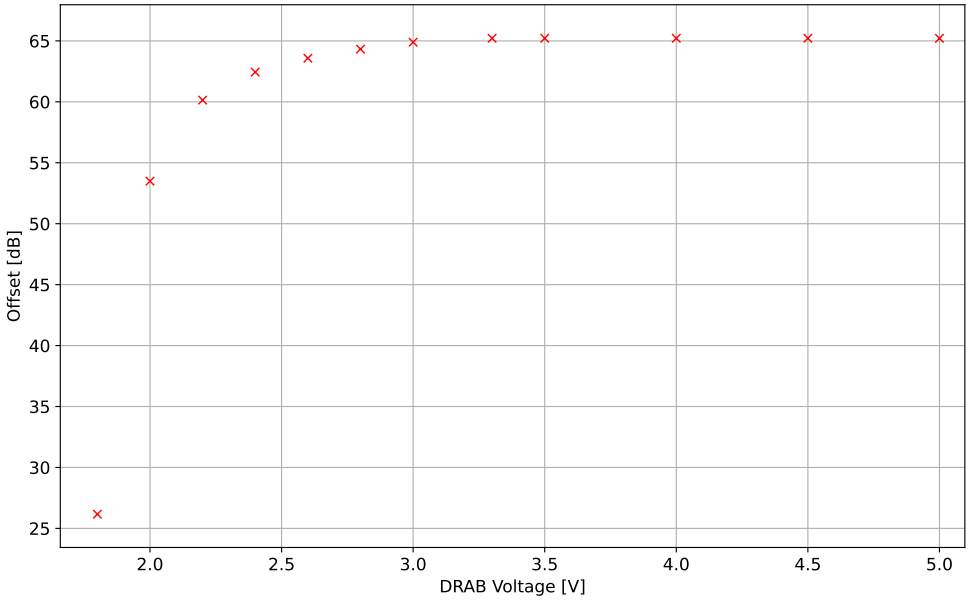

Figure 20: The offset of the linear fit at a frequency of 500 MHz versus the supply voltage of the DRAB board.

In summary, it can be said that if the supply voltage is above the minimum voltage, it has no influence on the gain of the boards. The minimum supply voltage for the IGLU board is 2.8 V and for the DRAB board between 3.0 V and 3.3 V.

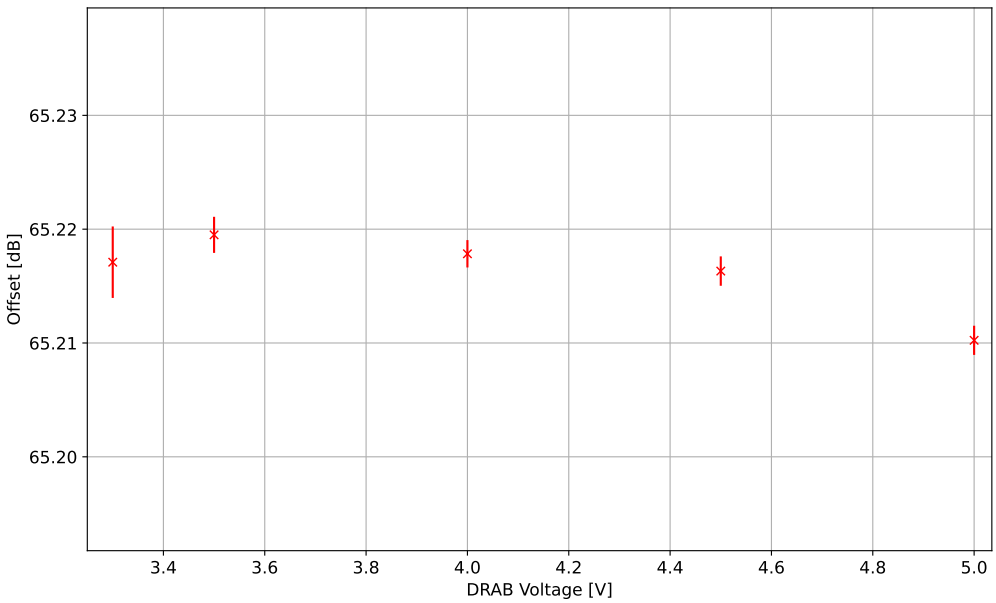

Figure 21: The offset of the linear fit at a frequency of 500 MHz versus the supply voltage of the DRAB board. Zoomed into the stable range above 3.3 V

4.5. Differences between different DRAB-Boards

Having previously only analyzed the properties of a single channel on a single DRAB board, different channels from different DRAB boards are now to be compared with each other. On the following DRAB boards all channels has been measured: C0038 (Ref DRAB), C0042, C0043, C0047, C0052, C0059, C0060 and C0065. Also, here a linear fit has been used to quantify the S_{21} parameter on each individual channel of each board. Here too, the selected frequency range is $460 - 550\,\mathrm{MHz}$, and a $f_0 = 500\,\mathrm{MHz}$ center frequency has been used. The parameters of the fits can be seen in Figure 22

From the fits the following statistical properties could be determined: The average gain at $f_0 = 500\,\mathrm{MHz}$ is $S_0 = 64.78 \pm 0.33\,\mathrm{dB}$ the average fitted slope is $m = -0.0112 \pm 0.0004\,\frac{\mathrm{dB}}{\mathrm{MHz}}$. Since each board is measured individually for modeling, these variations should not be a problem. These variations should be due to component tolerances within the DRAB boards, which are difficult to measure or name in detail.

One possible component that is simple to check is the internal voltage, which should be stabilized by the LDO to a voltage of 2.7V. However, this voltage is also subject to voltage fluctuations, due to tolerances of the LDO or the resistors in the voltage divider used to generate the reference voltage.

These voltage fluctuations could cause gain fluctuations of the amplifier ICs or of the photo diode, which is reverse biased by this voltage (see Figure 4). This voltage is therefore referred below as bias voltage. There are test pins on the board to measure the bias voltage, which is equal for all channels of the board. The bias voltage has been measured using an oscilloscope. Following bias voltages could be measured:

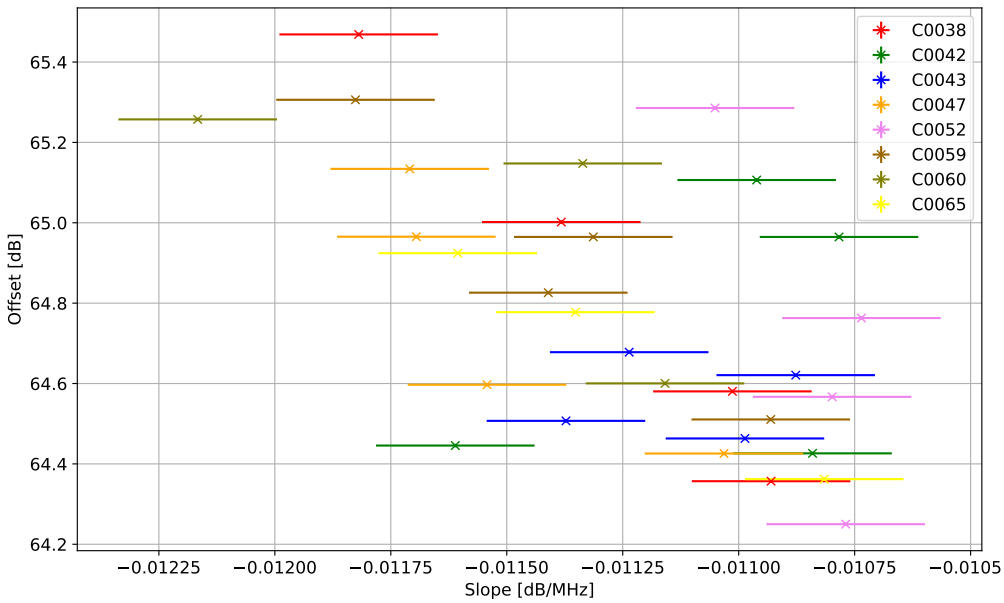

Figure 22: Fit parameters of linear fits on measured S_{21} parameters of different channels on different drab boards.

DRAB ID	Bias Voltage [V]
`Amp_DRAB_C0038`	2.693 ± 0.005
`Amp_DRAB_C0060`	2.692 ± 0.005
`Amp_DRAB_C0042`	2.711 ± 0.005
`Amp_DRAB_C0047`	2.691 ± 0.005
`Amp_DRAB_C0043`	2.701 ± 0.005
`Amp_DRAB_C0065`	2.700 ± 0.005
`Amp_DRAB_C0052`	2.699 ± 0.005
`Amp_DRAB_C0059`	2.718 ± 0.005

The bias voltage versus the gain offset is plotted in Figure 23. Although differences in the bias voltage could be measured between the boards, no correlation to the gain offset could be determined within the scope of the measurement accuracy. The fluctuations in the bias voltage therefore do not appear to have a major effect on the gain. It seems that the gain fluctuations are dominated by tolerances of other components in the boards.

4.6. Unusual Measurements

Unusual measurement results were obtained twice during the measurements on the VNA.

The first unusual measurement was a S_{11} parameter, which deviated significantly from the usual forms. Typical frequency responses of S_{11} are shown in Figure 24. Sometimes the S_{11} shows much higher values, with resonances at multiple frequencies. For this unusual measurement a simple solution could be found. It is caused by soiled SMA connectors at the IGLU input. The cable does have a gold-plated connector and the connector on the IGLU side is a more robust, nickel-plated connector. Repeatedly screwing and unscrewing the connector

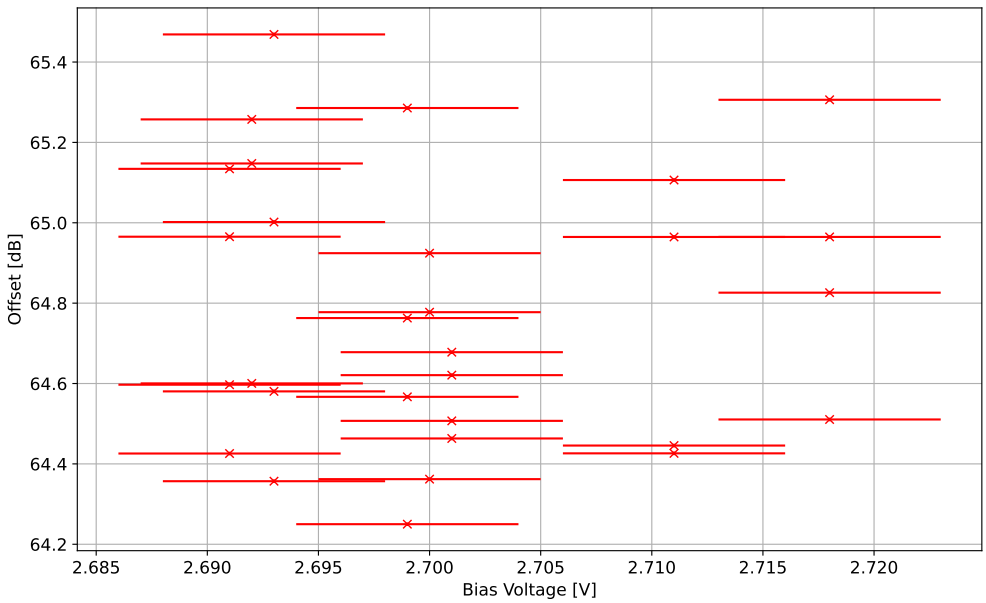

Figure 23: The internal (bias) voltage versus the offset of the linear fit. No dependence could be found.

will peel off small pieces of the gold-plating. These pieces can stick on the PTFE dielectric in the connector and change the impedance and therefore cause reflections. After cleaning the connector, the S_{11} parameter is normal again.

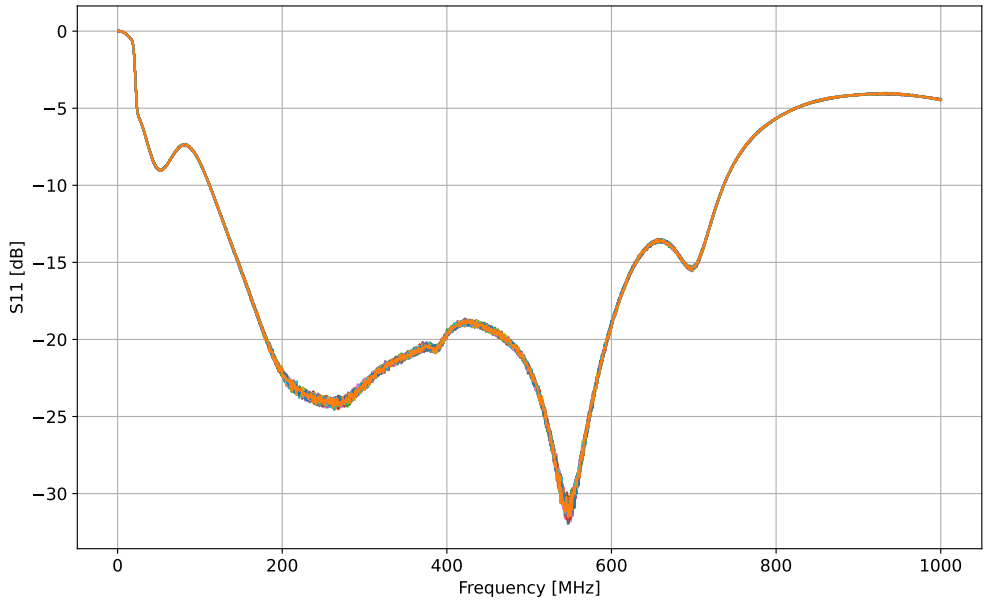

Figure 24: Typical frequency responses of S_{11} from different DRABs.

The second unusual measurement was a "distortion" of measured S_{21} parameters. During multiple measurements of the IGLU-fiber-DRAB chain, without changing or reconnecting of the boards, the S_{21} frequency responses deviated strongly, without apparent reason. These S_{21} measurements are plotted in Figure 25.

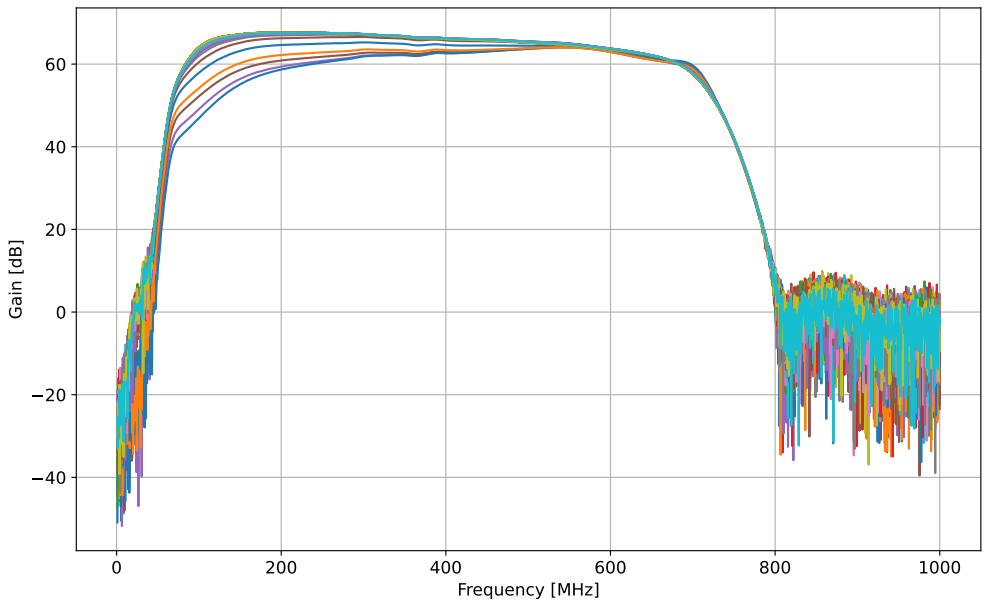

Figure 25: Distorted S_{21} measurements. The curves should look similar, but they are deviating significantly.

To analyze this phenomenon in more detail, the measured S_{21} parameter at 120 MHz was plotted over the sequence of the measurement. 120 MHz was taken because at this frequency the curves differ strongly. The results of this can be seen in Figure 26. You can see that this phenomenon normalizes with time. The time per measurement is about 1 minute, therefore this phenomenon normalized after about 10 minutes.

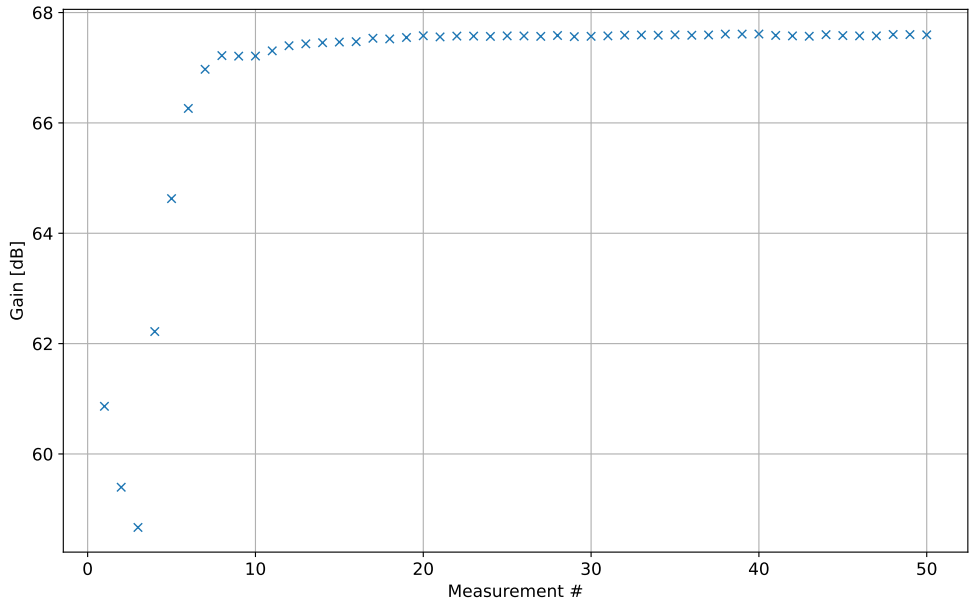

Figure 26: The distortion is time dependent and normalized after about 10 minutes.

Since the shape of this normalization curve corresponds to a curve that would be expected from a warm-up process, this phenomenon was compared with the warm-up process when the VNA is switched on. This is visible in Figure 27, however, the changes that occur here

are significantly smaller than those that occurred during the measurement. A cause of this phenomenon could not be found, and occurred only once.

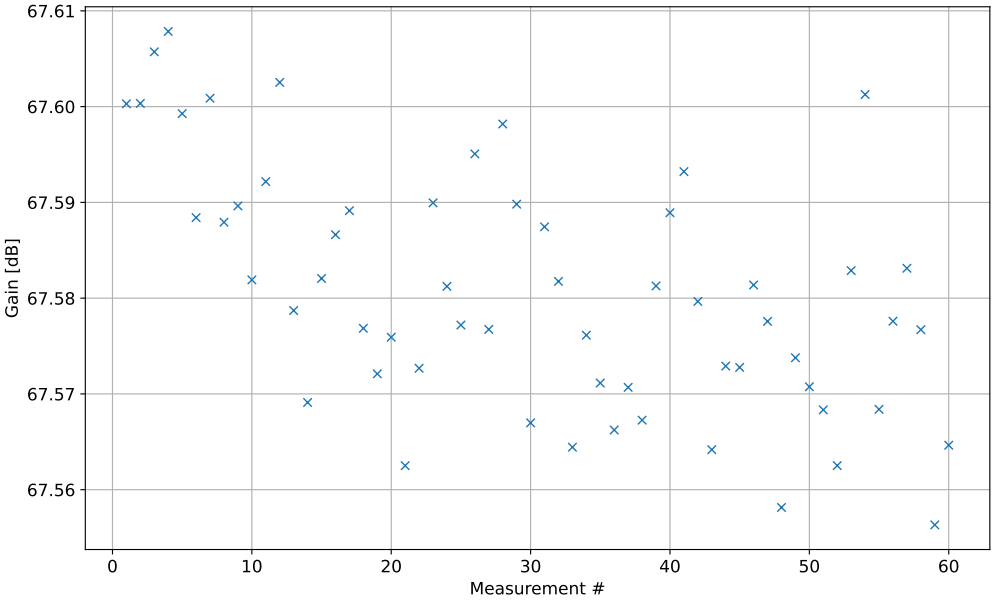

Figure 27: The warm-up phase showed much smaller variations than the strange phenomenon during the measurement series.

5. Conclusions

In this work, the reproducibility of calibration measurements of the IGLU fiber DRAB chain was analyzed. It was possible to improve the calibration of the VNA, which was used to measure the S-parameters. This was done by setting the output power of the ports to different values and by increasing the output power during the calibration of the VNA.
It was also shown that the reconnection of the SC connector between the fiber and the DRAB board affects the transmission characteristics of the entire chain. Fluctuations in the supply voltage, as long as they are above a certain minimum voltage, do not appear to influence the gain of the boards. Differences in gain have been found between different DRAB boards, but these have not been attributed to differences in internal supply voltage.

The results of this work mean that calibration measurements with the VNA can now be carried out with less noise. In addition, it was shown that future measurement setups where a high reproducibility of the gain is required should avoid SC connectors and use FC fiber connectors instead.

A. Appendix

A.1. Calibration Process

This is a step-by-step guide to perform an optimized calibration of the Tektronics P5020A VNA.

Open Sidebar

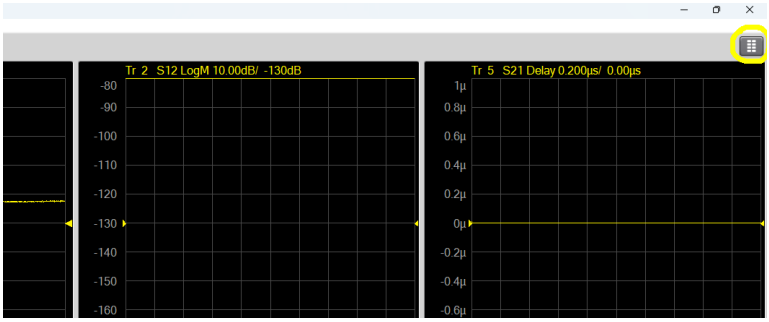

Figure 28

After opening the VNA-application, click in on the table icon in the top bar, to open the sidebar. This allows simple access to all further settings.

Setup measurements

Now you have to set which measurements are to be carried out and which sweep parameters should be used. If a so called "Status File" for the measurement is already available, this step can be skipped.
First delete all measurements which are shown in the application. This can done by clicking on each plot and click on the trash can icon in the top bar. Now the application should look like Figure 29.

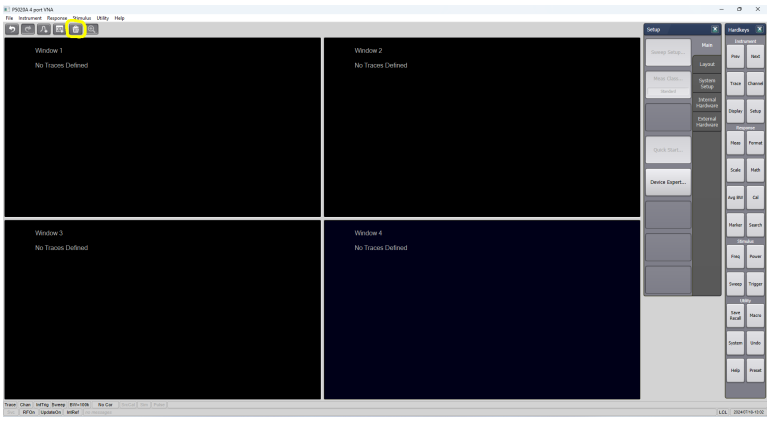

Figure 29

Now add the measurements which should be carried out. This can be done by clicking on the curve add icon in the top bar (see Figure 30).

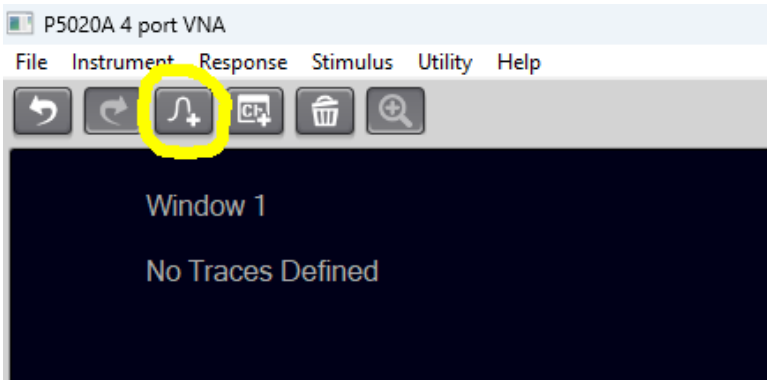

Figure 30

The created curve can be placed by clicking on one of the windows before adding it or by drag-and-drop the label of the curve onto another window (see Figure 31). While dragging over a window different quadrangles are visible. By dropping the the label on one of the trapezoids on the edges of each window, a new window is created on the corresponding side of the existing window.

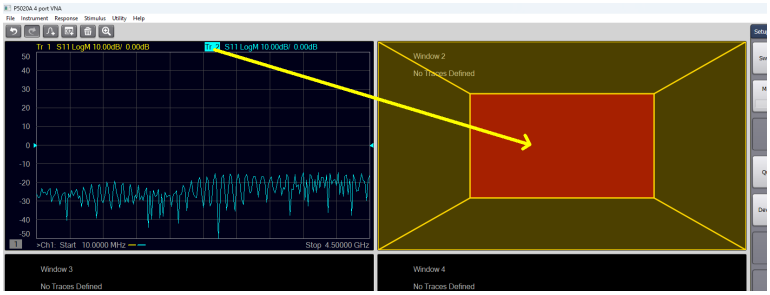

Figure 31

In total 5 measurements are needed: S_{11}, S_{12}, S_{21}, S_{22}, S_{21} (Group) Delay.
The phase measurements do not have to be created separately, it is sufficient to create only the magnitude measurements.
After adding five measurements the type can be set as follows: Click on the corresponding window, then navigate in the sidebar "Response" $\rightarrow$ "Meas" and set the type appropriately.

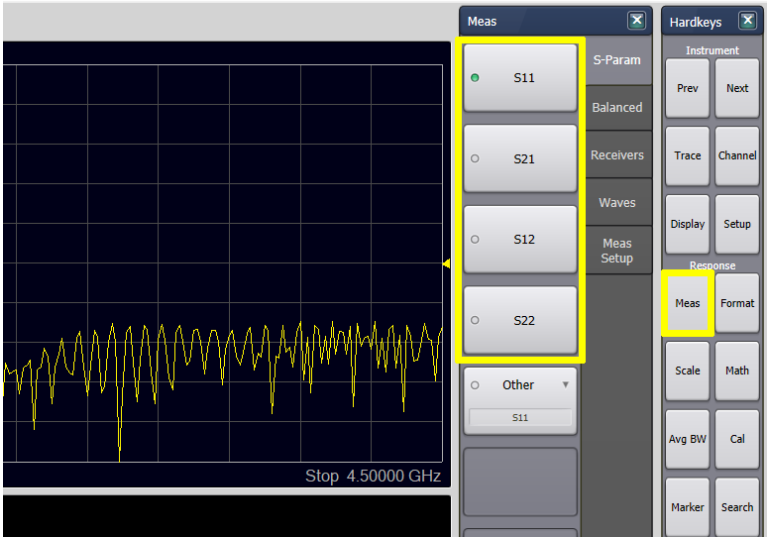

Figure 32

To set up the delay measurement, a additional step is required [21]: Set S_{21} as type and go to "Response" → "Format" and set format to "Delay" (see Figure 33).

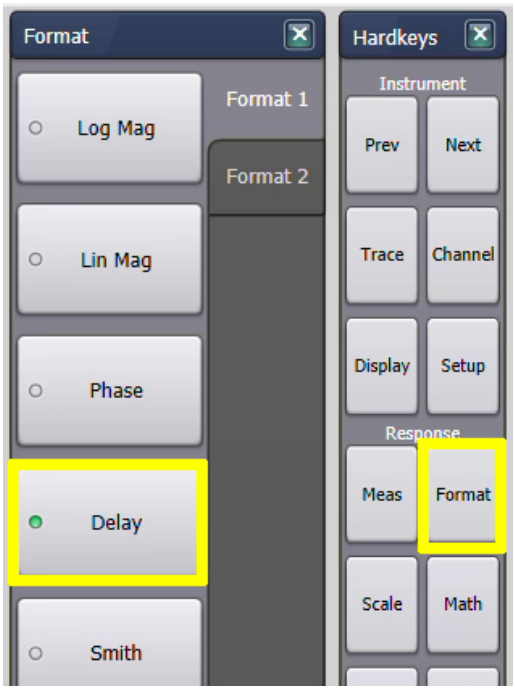

Figure 33

Finally the frequency sweep parameters must be set. In the sidebar go to "Instrument" → "Setup" → "Sweep Setup". Set the values in the opening window as shown in Figure 34.

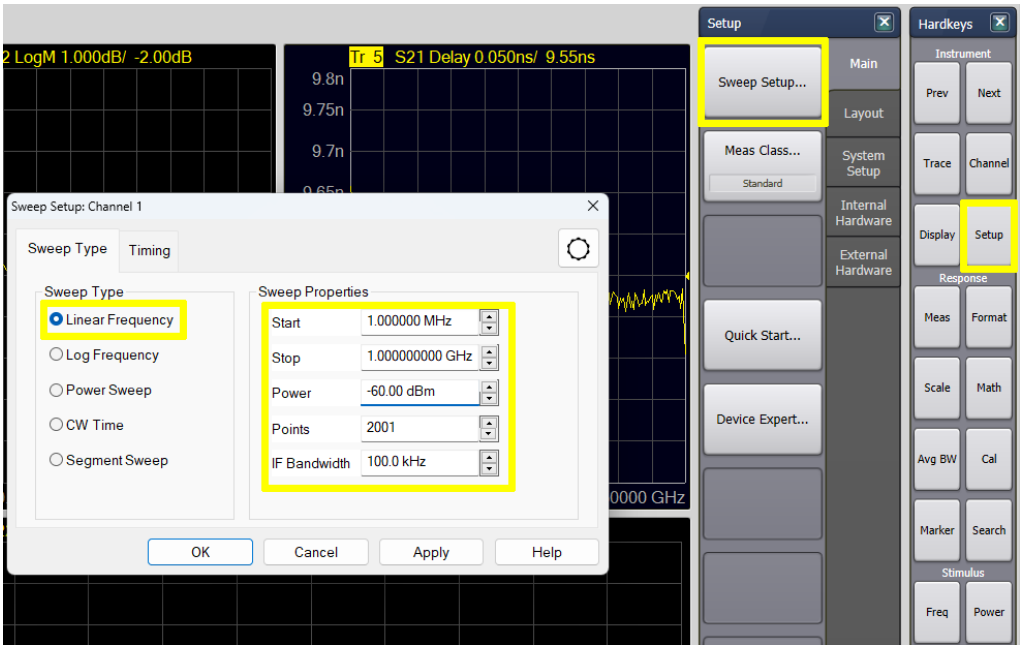

Figure 34

The created measurement structure can now be saved as a "Status-File" via "File" → "Save State As". To prevent to save any calibration settings at this point change the file extension to ".sta".

Load measurement settings

The "Status-File" can be loaded for future re-calibrations via "File" → "Recall State". This restores the measurement settings and drop any existing calibrations.

Set Ouput Power

Before starting the calibration the port output power and the port receiver gain must be set. To do this navigate in the sidebar to "Stimulus" → "Power". Here switch coupling to "OFF". Select port 1, click on power level and enter the port power, in the upper text box, by using the on screen keyboard. Do the same for port 2.
Optimal values are $P_{\text{Port1}} = -30\,\text{dBm}$ and $P_{\text{Port2}} = -10\,\text{dBm}$.

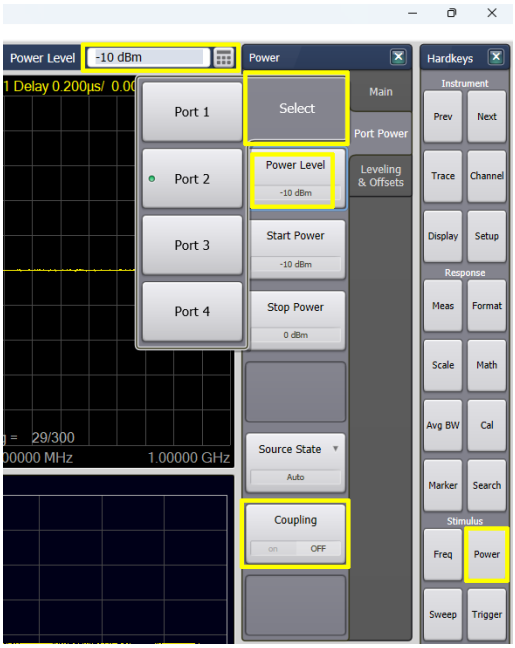

Figure 35

Next set the receiver gain for calibration. Go to “Instrument” → “Setup” → “Internal Hardware” → “Receiver Gain”. Set the values as shown in Figure 36.

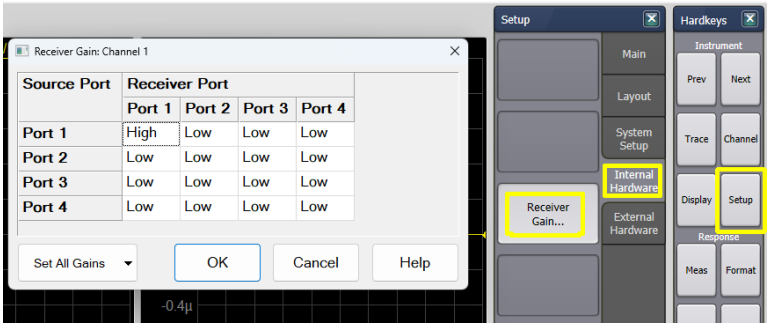

Figure 36

Set Averaging

To set the sweep averaging to to “Response” → “Avg BW”. Here click on “Averaging” and enter 300 using the upper text box and the on-screen keyboard. Make sure “Average Type” is set to “SWEEP”.

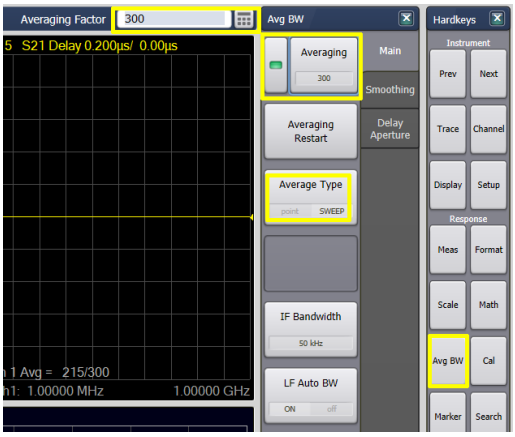

Figure 37

Start Calibration

Now connect the VNA ports to the ECAL and connect the ECAL via USB to the computer. It is automatically recognized which VNA port is connected to which ECAL port, a special assignment is not needed.
To start the calibration go to "Response" → "Cal" → "Other Cals" → "ECal". In the opening window select "2 Port Ecal". Then press next and measure.
The calibration starts now and will need about half an hour. During calibration no interaction is required.

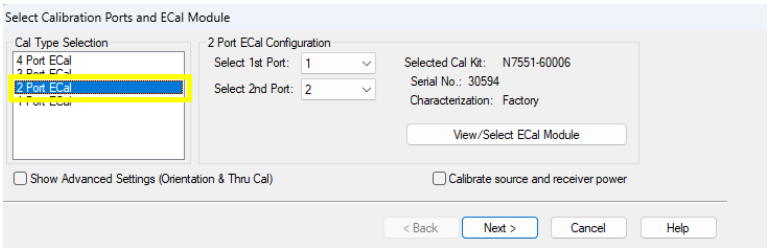

Figure 38

When calibration is finished a window appears were you can press finish.

Set Output Power

After the calibration the port output power must be reduced and the port receiver gain must be adapted. To do this navigate in the sidebar again to "Stimulus" → "Power".
Now set $P_{\text{Port1}} = -60\,\text{dBm}$ and $P_{\text{Port2}} = -10\,\text{dBm}$.

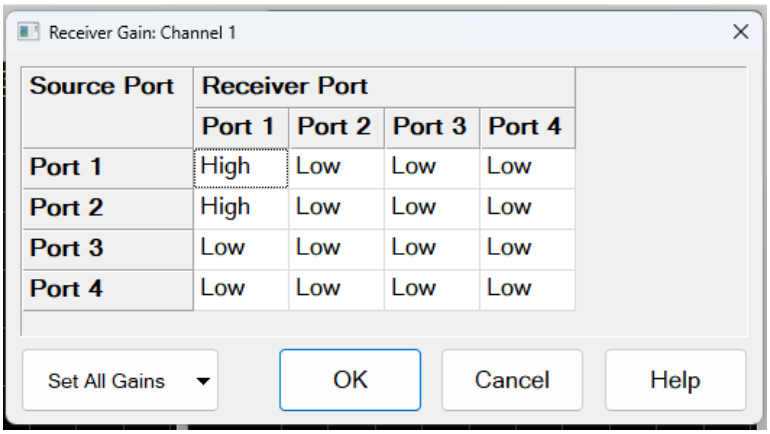

Figure 39

To adapt the receiver gain, go to "Instrument" → "Setup" → "Internal Hardware" → "Receiver Gain" and set the values according to Figure 39.

Save Calibration Data

Finally save the status and calibration to a CSA-file via "File" → "Save State As". Make sure to use the ".csa" file extension now, to save the calibration data.
The path to this file needs to be set in the measurement python script (see next section).

A.2. Python data retrieval script

This script can be used to save the measured data of the S_{xy} parameters and the group delay of each channel of the DRAB boards. It asks for a directory in which the data should be saved. Subdirectories are created for each DRAB in this directory. These subdirectories contain the measurement data. Each measured channel creates three CSV files:

- `{drab_id}_chan_{channel}_MA.csv`: This file contains the frequency dependent S_{xy} parameters as magnitude. See header for column definition. Second S_{21} is duplicate.
- `{drab_id}_chan_{channel}_DB.csv`: This file contains the frequency dependent S_{xy} parameters as decibel. See header for column definition. Second S_{21} is duplicate. This file has been used for most plots in this work.
- `{drab_id}_chan_{channel}_GroupDelay.csv`: This file contains the frequency dependent group delay. See header for column definition.

```
import pyvisa as visa
from time import sleep
import os
from tqdm import tqdm
import sys

#Base dir where data should be stored. User input will be relative to this
    directory.
BASEDIR = r"C:\Users\RNO-G\Desktop\DRAB_measurement"
```

```
#CSA setup/calibration file
CALFILE = r"C:\Users\RNO-G\Desktop\DRAB_measurement\Cal_06_13_-30-60-300.
    csa"

#Time to wait for averages to finish (seconds)
AVG_WAIT_TIME = 60


#Wait for user input that GUI has started
input("\nSwitch on VNA and open GUI. Press any key when done.")


#Init the VNA
try:
    rm = visa.ResourceManager('')
    vna=rm.open_resource('TCPIP0::DESKTOP-J67LMJ8::hislip0,4880::INSTR')
except:
    print(f"Oops! {sys.exc_info()[0]} occurred.")
    print("Could not connect to VNA")
    sys.exit()

sleep(1)

vnaid = vna.query('*IDN?').strip()
print(f"Connected to {vnaid}")


#Load calibration file
try:
    vna.write(f'MMEM:LOAD:CSAR "{CALFILE}"')
except:
    print('Had problems recalling setting file')
    sys.exit()


#Wait 10s
print("Wait for settings to be settled")
for t in tqdm(range(10)):
    sleep(1)


#Check if port power too high
try:
    ret=vna.query('SOUR:POW?').strip()
except:
    print(f"Oops! {sys.exc_info()[0]} occurred.")
    print('Had problems reading power')
    sys.exit()

print(f'RF Source Power is set to {ret}dBm\n')
if float(ret)>-40:
    print('Ouch, power to high.')
    sys.exit()


#Wait for user input confirm
```

```
input("Confirm that S-Parameter measurement is loaded and RF Output is set
    to -60dB. Press any key when done.")



#Enter directory where meausrements should be stored
path=input("Enter path for data to be stored: ")
if not os.path.exists(f'{BASEDIR}\\{path}'):
    os.mkdir(f'{BASEDIR}\\{path}')


print(f"Data is stored in {BASEDIR}\\{path}\\")

#Start measurement
try:
   while True:
      try:
         #Get the DRAB ID
         drab_id=input("Enter DRAB ID: ")
         drab_id=drab_id.strip()
         print(f"Commissioning DRAB {drab_id}")

         #Get S-parameters from each channel
         for chan in range(1,5):
            if chan==0:
               input("Connect channel 0 and power (output 2). Press any key
                   when done.")
            else:
               input(f"Connect channel {chan} and power. Press any key when
                   done.")


            doneflag=0
            while doneflag!=1:
               try:
                  vna.write('SENS:AVER:CLE')
                  print("Wait for Averages")
                  for t in tqdm(range(AVG_WAIT_TIME)):
                     sleep(1)

                  #Get data from GUI
                  vna.write(f'MMEM:STOR:DATA "{BASEDIR}\\{path}\\{drab_id}
                      _chan_{chan}_MA.csv","CSV Formatted Data","displayed
                      ","MA",-1')
                  vna.write(f'MMEM:STOR:DATA "{BASEDIR}\\{path}\\{drab_id}
                      _chan_{chan}_DB.csv","CSV Formatted Data","displayed
                      ","DB",-1')
                  vna.write(f'MMEM:STOR:DATA "{BASEDIR}\\{path}\\{drab_id}
                      _chan_{chan}_GroupDelay.csv","CSV Formatted Data","
                      Trace","displayed",5')
                  doneflag=1

               #Handle Keyboard Interrupt if measurement not finished
               except KeyboardInterrupt:
                  print(f"Oops! {sys.exc_info()[0]} occurred.")
                  input("I will do the channel again, please press any key
```

```
                    ")
            print("Done!")

      #Handle Keyboard Interrupt between measurements.
      except KeyboardInterrupt:
         print(f"Oops! {sys.exc_info()[0]} occurred.")
         ret=""
         while ret!='l' and ret!="n":
            ret=input("Leave (l) or next DRAB (n)? ")
            print(ret,type(ret))

         if ret=="l":
            print("Done, please exit VNA GUI and switch off")
            sys.exit()
         elif ret=="n":
            print('ok next')


except:
   print(f"Oops! {sys.exc_info()[0]} occurred.")
   print("Done, please exit VNA GUI and switch off")
   while True:
      sleep(1)
```

B. Bibliography

[1] M. G. Aartsen et al. "First Observation of PeV-Energy Neutrinos with IceCube". In: *Physical Review Letters* 111.2, 021103 (July 2013), p. 021103. DOI: 10.1103/PhysRevLett.111.021103. arXiv: 1304.5356 [astro-ph.HE].

[2] J. A. Aguilar et al. "Design and sensitivity of the Radio Neutrino Observatory in Greenland (RNO-G)". In: *Journal of Instrumentation* 16.3, P03025 (Mar. 2021), P03025. DOI: 10.1088/1748-0221/16/03/P03025. arXiv: 2010.12279 [astro-ph.IM].

[3] S. Aiello et al. "Sensitivity of the KM3NeT/ARCA neutrino telescope to point-like neutrino sources". In: *Astroparticle Physics* 111 (Sept. 2019), pp. 100–110. DOI: 10.1016/j.astropartphys.2019.04.002. arXiv: 1810.08499 [astro-ph.HE].

[4] Anita Collaboration et al. "The Antarctic Impulsive Transient Antenna ultra-high energy neutrino detector: Design, performance, and sensitivity for the 2006-2007 balloon flight". In: *Astroparticle Physics* 32.1 (Aug. 2009), pp. 10–41. DOI: 10.1016/j.astropartphys.2009.05.003. arXiv: 0812.1920 [astro-ph].

[5] Ara Collaboration et al. "Design and initial performance of the Askaryan Radio Array prototype EeV neutrino detector at the South Pole". In: *Astroparticle Physics* 35.7 (Feb. 2012), pp. 457–477. DOI: 10.1016/j.astropartphys.2011.11.010. arXiv: 1105.2854 [astro-ph.IM].

[6] G.A. Askar'yan. "Coherent Radio Emission from Cosmic Showers in Air and in Dense Media". In: *Soviet Journal of Experimental and Theoretical Physics* 21 (Sept. 1965), p. 658.

[7] S. W. Barwick et al. "Design and Performance of the ARIANNA HRA-3 Neutrino Detector Systems". In: *IEEE Transactions on Nuclear Science* 62.5 (2015), pp. 2202–2215. DOI: 10.1109/TNS.2015.2468182.

[8] V. S. Beresinsky and Georgii Timofeevich Zatsepin. "Cosmic rays at ultra high energies (neutrino?)" In: *Physics Letters B* 28 (1969), pp. 423–424. URL: https://api.semanticscholar.org/CorpusID:122576177.

[9] P. W. Gorham et al. "Observations of the Askaryan Effect in Ice". In: *Physical Review Letters* 99.17, 171101 (Oct. 2007), p. 171101. DOI: 10.1103/PhysRevLett.99.171101. arXiv: hep-ex/0611008 [hep-ex].

[10] Steffen Hallmann et al. "Sensitivity studies for the IceCube-Gen2 radio array". In: *arXiv e-prints*, arXiv:2107.08910 (July 2021), arXiv:2107.08910. DOI: 10.48550/arXiv.2107.08910. arXiv: 2107.08910 [astro-ph.HE].

[11] Francis Halzen and Dan Hooper. "High-energy neutrino astronomy: the cosmic ray connection". In: *Reports on Progress in Physics* 65.7 (July 2002), pp. 1025–1078. DOI: 10.1088/0034-4885/65/7/201. arXiv: astro-ph/0204527 [astro-ph].

[12] KEYSIGHT. *Applying Error Correction to Vector Network Analyzer Measurements*. URL: https://www.keysight.com/us/en/assets/7018-06761/application-notes/5965-7709.pdf.

[13] KEYSIGHT. *Streamline Series Vector Network Analyzer (A-models) - Datasheet*. URL: https://www.keysight.com/de/de/assets/7018-06469/data-sheets/5992-3606.pdf.

[14] KEYSIGHT. *VNA Issues - Understanding High Gain Power Amplifier Measurement Considerations*. URL: https://technicalsupport.keysight.com/vna-issues-understanding-high-power-amplifier-measurement-considerations.

[15] Eric Oberla. *DRAB schematics RevD*.

[16] Eric Oberla. *IGLU schematics RevG*.

[17] Eric Oberla et al. "Low-Power Radiofrequency Systems for the RNO-G Project". In: July 2023. DOI: 10.22323/1.444.1171.

[18] Prof. Dr. Ing. Obermann. *S-Parameter 1*. YouTube. URL: https://www.youtube.com/watch?v=2p16kZR-2E0.

[19] Christian Glaser Steven W. Barwick. "Radio Detection of High Energy Neutrinos in Ice". In: *Encyclopedia of Cosmology II*.

[20] Tektronix. *Introduction to VNA Basics*. URL: https://download.tek.com/document/70W_60918_0_Tek_VNA_PR.pdf.

[21] Tektronix. *Making Phase and Group Delay Measurements with the TTR500 VNA*. URL: https://www.tek.com/de/video/how-to/making-phase-and-group-delay-measurements-with-the-ttr500-vna.

Eidesstattliche Erklärung

Hiermit versichere ich, dass ich die vorliegende Arbeit selbständig und ohne unerlaubte Hilfsmittel verfasst habe. Ich habe keine anderen als die angegebenen Quellen und Hilfsmittel benutzt und alle wörtlich oder dem Sinn nach aus anderen Texten entnommenen Stellen als solche kenntlich gemacht. Dies gilt für gedruckte Texte wie für Texte aus dem Internet. Die Arbeit wurde in der vorliegenden bzw. modifizierten Form noch keiner anderen Stelle zur Prüfung vorgelegt und dieselbe hat auch nicht anderen Zwecken - auch nicht teilweise - gedient. Mit einer Plagiatsprüfung bin ich einverstanden. Mir ist bewusst, dass jeder Verstoß gegen diese Erklärung eine Bewertung der eingereichten Arbeit mit Note "ungenügend" zur Folge hat.

Erlangen, August 17, 2024 _____